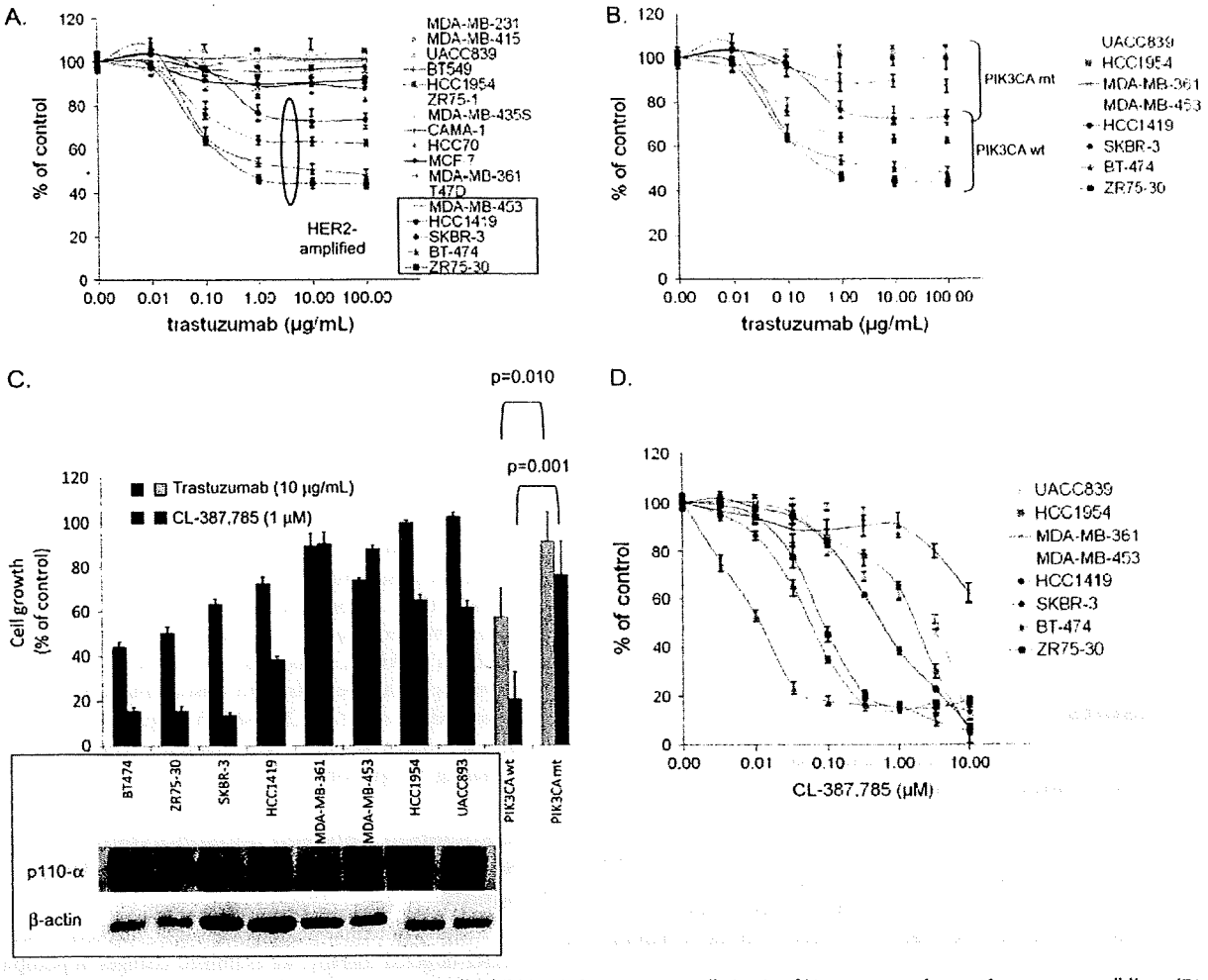

Figure 2. Effect of trastuzumab and CL-387,785 on growth inhibition in breast cancer cells *in vitro* [(A) trastuzumab on 17 breast cancer cell lines; (B) and (D) trastuzumab and CL-387,785 on eight *HER2*-amplified cell lines, respectively]. Breast cancer cells were grown in 10% serum-containing media for 5 days in the presence of various concentrations of trastuzumab (A and B) or CL-387,785 (D). The percentage of viable cells is shown relative to that of the untreated control and plotted on the *y*-axis, whereas trastuzumab and CL-387,785 concentrations are plotted on the *x*-axis. Each data point represents the mean value and standard deviation of 6–12 replicate wells. (C, top) Mean percentage of control and standard deviation of 6–12 replicate wells treated with 10 μg/ml trastuzumab and 1 μM CL-387,785, as well as those of *PIK3CA*-wild-type and -mutant cell lines (bottom), were plotted. (C, bottom) Protein expression of p110-α in *HER2*-amplified breast cancer cells. Blots were stripped and re-probed for β-actin as loading control.

Phosphorylation signals were then quantified and correlated with growth inhibition caused by trastuzumab and CL-387,785. As shown in Figure 4B, the closest association was observed between phospho-S6K changes and growth inhibition caused by trastuzumab and CL-387,785 [correlation coefficient (r), 0.811]. Further, close associations between phospho-S6K and cell growth were consistent when analyzed for trastuzumab and CL-387,785 separately (r for phospho-S6K versus growth: 0.8487 and 0.6970 for trastuzumab and CL-387,785, respectively).

dependency of *HER2*-amplified breast cancer cells on PI3K pathway

Given that inhibition of the PI3K pathway is critical in distinguishing cells sensitive from resistant to HER2-targeted agents (Figure 4B), we evaluated cell lines for the effects of LY294002, a PI3K inhibitor. As shown in Figure 5A, with the exception of ZR75-30, LY294002 induced a >30% growth inhibition compared with control in all cell lines. No significant difference in LY294002 sensitivity was observed between *PIK3CA*-mutant and -wild-type cell lines (Figure 5; $P = 0.655$). These results indicate that most *HER2*-amplified cells at least partly depend on the PI3K pathway regardless of the presence or absence of *PIK3CA* hotspot mutations.

To further gain insight into this concept, we evaluated phosphorylation levels of Akt and ERK1/2 in protein extracts obtained from cells under serum-starved conditions for 24 h. As shown in Figure 5B, despite the absence of serum factors, all *HER2*-amplified breast cancer cells showed a high level of phospho-Akt, regardless of *PIK3CA* genotype. High levels of phospho-Akt were also observed in MDA-MB-468, which lacks PTEN [30], and T47D, which harbors a *PIK3CA* mutation

(H1047R) [14]. These two cell lines do not show *HER2* amplification [23]. In contrast, no significant levels of phospho-Akt were observed in MDA-MB-231 and MDA-MB-435S, which show no *HER2* amplification, *PIK3CA* mutation, or PTEN loss [14, 23]. Further, with the exception of MDA-MB-231, all cell lines showed very low levels of phospho-ERK1/2 under serum-starved conditions. MDA-MB-231, in particular, was reported to contain double activating mutations in KRAS (G13D) and BRAF (G464V), whereas MDA-MB-435S showed an activating mutation in BRAF alone (V600E) [31]. These findings further support the concept that *HER2*-amplified cells tend to have HER2-PI3K signaling axis and they are thus dependent on the PI3K pathway rather than on extracellular signal-regulated kinase pathway.

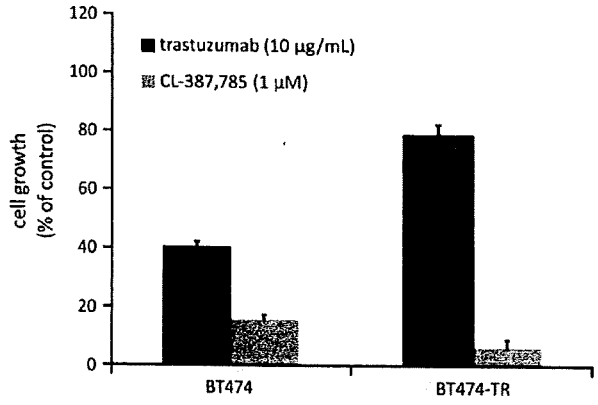

Figure 3. Effect of trastuzumab and CL-387,785 on growth inhibition in BT-474 and BT474-TR cells. Mean percentage of control and standard deviation of 6–12 replicate wells treated with 10 μg/ml trastuzumab and 1 μM CL-387,785 were plotted. BT474-TR remains sensitive to CL-387,785.

discussion

In this study, we show that gain-of-function mutations in *PIK3CA* genes are associated with trastuzumab resistance in naturally derived breast cancer cell lines showing *HER2* amplification. This finding is consistent with a recent study by Berns et al. [19] reporting trastuzumab resistance in SKBR-3 cells transfected with mutant *PIK3CA* (H1047R) compared with GFP control. Transfection of wild-type *PIK3CA*, however, appeared to equally cause trastuzumab resistance [19]. This observation does not identify either quantitative or qualitative changes in *PIK3CA* mutation as the major factor in developing trastuzumab resistance. In the present study, no clear association was observed between *PIK3CA* protein (p110-α) expression levels and *in vitro* sensitivity to trastuzumab

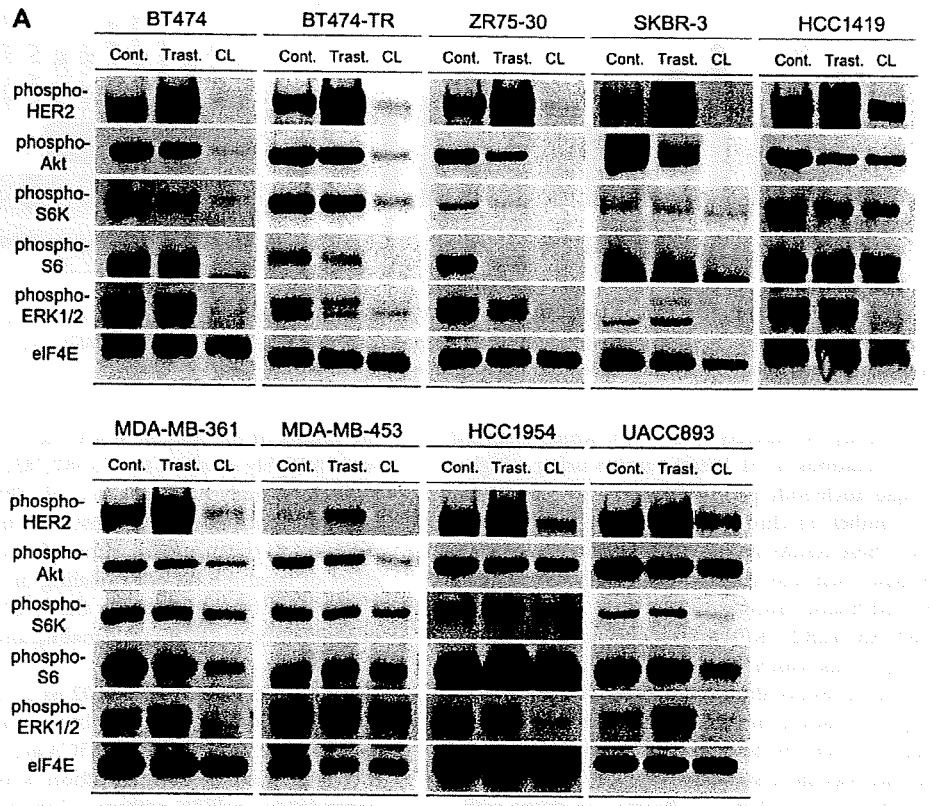

Figure 4. (A) Expression of phosphorylated-HER2, -Akt, -S6K, -S6 and -ERK1/2 in HER2-amplified breast cell lines with and without treatment with trastuzumab (10 μg/ml) and CL-387,785 (1 μM). Breast cell lines grown in 10% serum-containing media were lysed and immunoblotted for each protein. Blots were stripped and re-probed for eIF4E as loading control.

doi:10.1093/annonc/mdp304

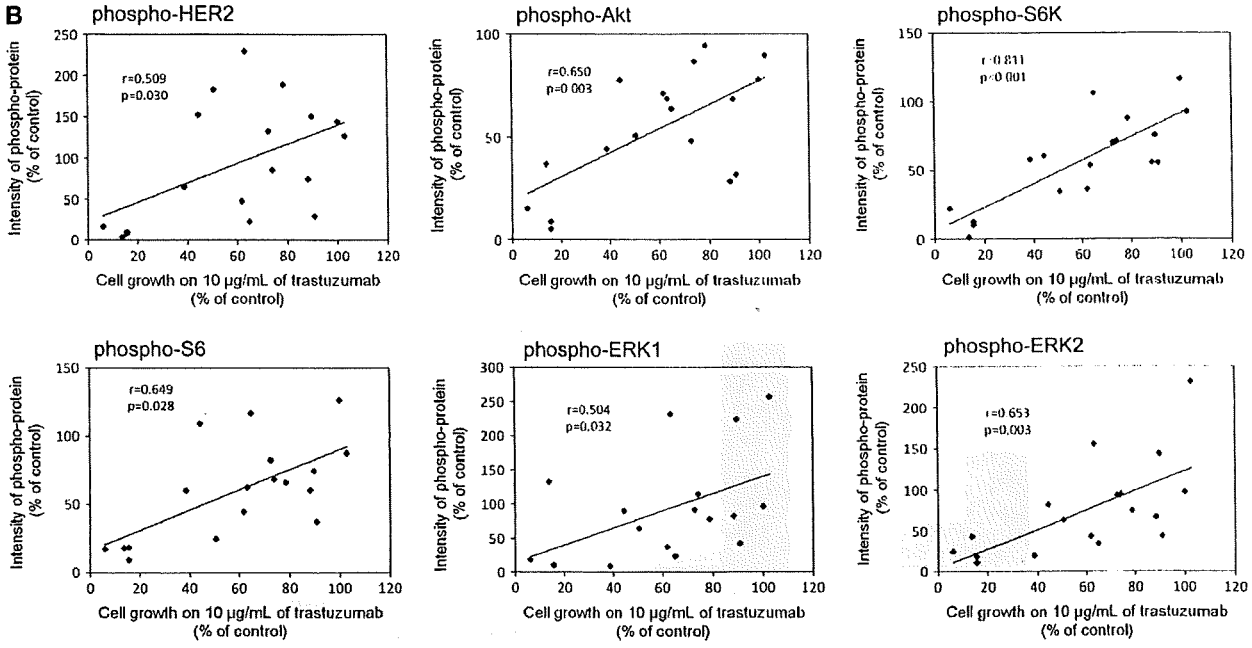

Figure 4. (Continued) (B) Correlation between changes in phosphorylation of HER2 signaling molecules and cell growth. Immunoblot quantification was carried out by densitometry using ImageJ software. Correlations were analyzed by calculating Pearson's correlation coefficient.

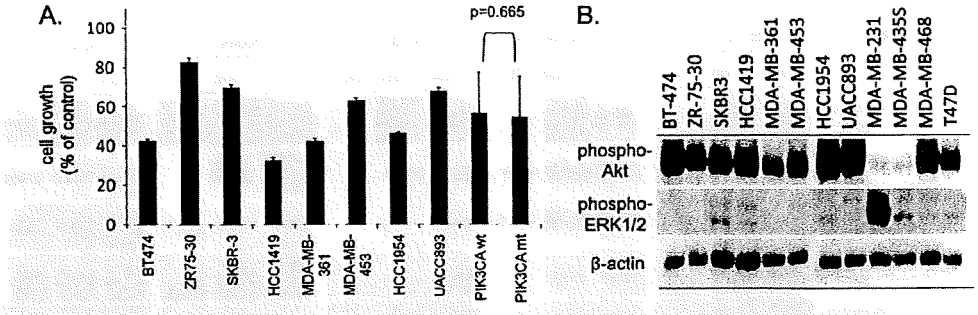

Figure 5. (A) Effect of LY294002 on growth inhibition in HER2-amplified breast cancer cell lines. Mean percentage of control and standard deviation of 6–12 replicate wells treated with 10 μM LY294002 were plotted. (B) Protein expression of phospho-Akt and phospho-ERK1/2 in HER2-amplified breast cancer cells under serum-starved condition. Blots were stripped and re-probed for β-actin as loading control.

(Figure 2C). A study by Haverty et al. [32], which analyzed copy number alterations in 51 breast tumors using a high-resolution single nucleotide polymorphism array, showed no gain in copy number on chromosome 3p, the location of the *PIK3CA* gene. These results indicate that qualitative changes in the *PIK3CA* gene itself may cause trastuzumab resistance in naturally derived breast cancer cells.

The CL-387,785 HER2-TKI was first evaluated to identify groups of compounds which may overcome trastuzumab resistance. Of note, results show an association between *PIK3CA* hotspot mutations and CL-387,785 resistance. Further, the difference in sensitivity between *PIK3CA*-wild-type and -mutant cell lines was more significant for CL-387,785 than for trastuzumab (Figure 2C). These results are consistent with a recent study by Eichhorn et al. [22], which showed that transfection of mutant *PIK3CA* (H1047R) in BT474 cells, which are sensitive to lapatinib, results in drug resistance. In contrast, the results of the present study show that BT474-TR cells remain highly sensitive to CL-387,785, which is consistent with a previous study by Konecny et al. [20] which reported that lapatinib remains active against cell lines selected by long-term exposure to trastuzumab. Although the study did not show the effect of lapatinib on cell signaling in secondary resistant cells, our present findings indicate that BT474-TR remains dependent on HER2/PI3K signaling and sensitive to HER2-TKI (Figure 4A).

We then evaluated LY294002 as a model PI3K inhibitor. Results show that *HER2*-amplified cells are generally sensitive to LY294002 regardless of *PIK3CA* genotype (Figure 5A), which indicates that *HER2* amplification is associated with dependency on PI3K pathway. Supporting this notion, all *HER2*-amplified breast cancer cells have high level of phosphorylation of Akt even in serum-starved condition. The Akt phosphorylation levels observed in *HER2*-amplified cells

were equivalent to those in MDA-MB-468 and T47D cells, which were reported to contain PTEN loss and a *PIK3CA* hotspot mutation without *HER2* amplification, respectively [23]. These findings therefore indicated that *HER2* amplification itself may have equivalent biological effect on PI3K signaling with PTEN loss or *PIK3CA* hotspot mutation. In addition, our results are consistent with a recent study by Oda et al. [33], in which they showed that HER2 and/or HER3 overexpression, PTEN, or *PIK3CA* mutations occur almost exclusively in breast and other cancer cell lines.

Findings in past and present studies may potentially lead to beneficial clinical applications. For *HER2*-amplified breast cancer showing no *PIK3CA* mutations, trastuzumab is likely to be effective, with possible rescue using HER2-TKIs in cases of relapse. For *HER2*-amplified breast cancer with *PIK3CA* mutations, inhibitors against molecules of the PI3K pathway are possibly more effective than anti-HER2 agents, which are unlikely to be beneficial.

In addition to pharmacogenetic approaches, including *PIK3CA* genotyping, pharmacodynamic markers are potentially powerful tools in individualized use of molecularly targeted therapy. In a number of previous pharmacodynamic studies on HER2- or EGFR-targeted therapy, phospho-Akt was used as a surrogate marker for PI3K pathway activity [34, 35]. In the present study, however, growth inhibition is more closely associated with changes in phospho-S6K than that in phospho-Akt. These findings indicate that the prediction of tumor response to trastuzumab may strongly benefit from measurements of S6K phosphorylation levels. The cause of the discrepancy between the association of cell growth with phospho-Akt and that with phospho-S6K, however, remains unclear. It may be due to the difference in sensitivity of phospho-specific antibodies used in the present study or the higher sensitivity of phospho-Akt to positive feedback signals following initial inhibition of the PI3K pathway compared with phospho-S6K.

The present study shows several limitations. First, although a relatively large panel of *HER2*-amplified breast cancer cell lines ($N = 8$) were used, the properties of all HER2-overexpressing breast tumors are not necessarily represented. Despite HER2 amplification being retained, particular tumor subtypes may have been selected in the establishment of cell lines. Secondly, in addition to inhibition of HER2 signaling, a few studies have indicated the contribution of antigen-dependent cellular cytotoxicity (ADCC) in the antitumor effect of trastuzumab. Because ADCC only works in *in vivo* conditions, our current data do not necessarily deny the potential effect of trastuzumab on tumors showing *PIK3CA* mutations [36]. Thirdly, although wild-type *PIK3CA* appeared necessary for trastuzumab sensitivity *in vitro*, other factors may be involved, as shown by results showing moderate resistance of HCC1419 to trastuzumab (Figure 2C). The mechanisms of *PIK3CA*-unrelated resistance remain unknown but are under current investigation in our laboratory.

In conclusion, our findings show an association between the presence of *PIK3CA* hotspot mutations and resistance to not only trastuzumab but also HER2-TKI in naturally derived *HER2*-amplified breast cancer cell lines. Further, PI3K inhibitors are potentially effective in overcoming trastuzumab resistance caused by *PIK3CA* mutations. Assessment of S6K phosphorylation levels may be a useful pharmacodynamic marker correlated to the antitumor effect of HER2-targeted therapy. A better understanding of these findings, however, may require further investigation in clinical trials and concomitant translational studies.

funding

Grant-in-Aid for Young Scientists (B) from Ministry of Education, Culture, Sports, Science and Technology of Japan to T.M.; AstraZeneca Research Grant 2007 to T.M.; Kobe University Medical School Research Grant for Young Scientists to T.M.; Grants-in-Aid for Cancer Research from Ministry of Health, Labor and Welfare of Japan to H.M.

references

1. McPherson K, Steel CM, Dixon JM. ABC of breast diseases. Breast cancer-epidemiology, risk factors, and genetics. BMJ 2000; 321: 624–628.
2. Parkin DM, Bray F, Ferlay J, Pisani P. Global cancer statistics, 2002. CA Cancer J Clin 2005; 55: 74–108.
3. Slamon DJ, Godolphin W, Jones LA et al. Studies of the HER-2/neu proto-oncogene in human breast and ovarian cancer. Science 1989; 244: 707–712.
4. Slamon DJ, Clark GM, Wong SG et al. Human breast cancer: correlation of relapse and survival with amplification of the HER-2/neu oncogene. Science 1987; 235: 177–182.
5. Slamon DJ, Leyland-Jones B, Shak S et al. Use of chemotherapy plus a monoclonal antibody against HER2 for metastatic breast cancer that overexpresses HER2. N Engl J Med 2001; 344: 783–792.
6. Piccart-Gebhart MJ, Procter M, Leyland-Jones B et al. Trastuzumab after adjuvant chemotherapy in HER2-positive breast cancer. N Engl J Med 2005; 353: 1659–1672.
7. Romond EH, Perez EA, Bryant J et al. Trastuzumab plus adjuvant chemotherapy for operable HER2-positive breast cancer. N Engl J Med 2005; 353: 1673–1684.
8. Buzdar AU, Ibrahim NK, Francis D et al. Significantly higher pathologic complete remission rate after neoadjuvant therapy with trastuzumab, paclitaxel, and epirubicin chemotherapy: results of a randomized trial in human epidermal growth factor receptor 2-positive operable breast cancer. J Clin Oncol 2005; 23: 3676–3685.
9. Vogel CL, Cobleigh MA, Tripathy D et al. Efficacy and safety of trastuzumab as a single agent in first-line treatment of HER2-overexpressing metastatic breast cancer. J Clin Oncol 2002; 20: 719–726.
10. Scaltriti M, Rojo F, Ocana A et al. Expression of p95HER2, a truncated form of the HER2 receptor, and response to anti-HER2 therapies in breast cancer. J Natl Cancer Inst 2007; 99: 628–638.
11. Xia W, Liu LH, Ho P, Spector NL. Truncated ErbB2 receptor (p95ErbB2) is regulated by heregulin through heterodimer formation with ErbB3 yet remains sensitive to the dual EGFR/ErbB2 kinase inhibitor GW572016. Oncogene 2004; 23: 646–653.
12. Nagata Y, Lan KH, Zhou X et al. PTEN activation contributes to tumor inhibition by trastuzumab, and loss of PTEN predicts trastuzumab resistance in patients. Cancer Cell 2004; 6: 117–127.
13. Samuels Y, Wang Z, Bardelli A et al. High frequency of mutations of the PIK3CA gene in human cancers. Science 2004; 304: 554.
14. Saal LH, Holm K, Maurer M et al. PIK3CA mutations correlate with hormone receptors, node metastasis, and ERBB2, and are mutually exclusive with PTEN loss in human breast carcinoma. Cancer Res 2005; 65: 2554–2559.
15. Campbell IG, Russell SE, Choong DY et al. Mutation of the PIK3CA gene in ovarian and breast cancer. Cancer Res 2004; 64: 7678–7681.
16. Lee JW, Soung YH, Kim SY et al. PIK3CA gene is frequently mutated in breast carcinomas and hepatocellular carcinomas. Oncogene 2005; 24: 1477–1480.
17. Isakoff SJ, Engelman JA, Irie HY et al. Breast cancer-associated PIK3CA mutations are oncogenic in mammary epithelial cells. Cancer Res 2005; 65: 10992–11000.

18. Gymnopoulos M, Elsliger MA, Vogt PK. Rare cancer-specific mutations in PIK3CA show gain of function. Proc Natl Acad Sci U S A 2007; 104: 5569–5574.
19. Berns K, Horlings HM, Hennessy BT et al. A functional genetic approach identifies the PI3K pathway as a major determinant of trastuzumab resistance in breast cancer. Cancer Cell 2007; 12: 395–402.
20. Konecny GE, Pegram MD, Venkatesan N et al. Activity of the dual kinase inhibitor lapatinib (GW572016) against HER-2-overexpressing and trastuzumab-treated breast cancer cells. Cancer Res 2006; 66: 1630–1639.
21. Cameron D, Casey M, Press M et al. A phase III randomized comparison of lapatinib plus capecitabine versus capecitabine alone in women with advanced breast cancer that has progressed on trastuzumab: updated efficacy and biomarker analyses. Breast Cancer Res Treat 2008; 112: 533–543.
22. Eichhorn PJ, Gili M, Scaltriti M et al. Phosphatidylinositol 3-kinase hyperactivation results in lapatinib resistance that is reversed by the mTOR/phosphatidylinositol 3-kinase inhibitor NVP-BEZ235. Cancer Res 2008; 68: 9221–9230.
23. Lacroix M, Leclercq G. Relevance of breast cancer cell lines as models for breast tumours: an update. Breast Cancer Res Treat 2004; 83: 249–289.
24. Mukohara T, Shimada H, Ogasawara N et al. Sensitivity of breast cancer cell lines to the novel insulin-like growth factor-1 receptor (IGF-1R) inhibitor NVP-AEW541 is dependent on the level of IRS-1 expression. Cancer Lett 2009; 282: 14–24.
25. Discafani CM, Carroll ML, Floyd MB Jr et al. Irreversible inhibition of epidermal growth factor receptor tyrosine kinase with in vivo activity by N-[4-[(3-bromophenyl)amino]-6-quinazolinyl]-2-butynamide (CL-387,785). Biochem Pharmacol 1999; 57: 917–925.
26. Zhang H, Liu G, Dziubinski M et al. Comprehensive analysis of oncogenic effects of PIK3CA mutations in human mammary epithelial cells. Breast Cancer Res Treat 2008; 112: 217–227.
27. Burris HA III, Hurwitz HI, Dees EC et al. Phase I safety, pharmacokinetics, and clinical activity study of lapatinib (GW572016), a reversible dual inhibitor of epidermal growth factor receptor tyrosine kinases, in heavily pretreated patients with metastatic carcinomas. J Clin Oncol 2005; 23: 5305–5313.
28. Shimamura T, Li D, Ji H et al. Hsp90 inhibition suppresses mutant EGFR-T790M signaling and overcomes kinase inhibitor resistance. Cancer Res 2008; 68: 5827–5838.
29. Koivunen JP, Mermel C, Zejnullahu K et al. EML4-ALK fusion gene and efficacy of an ALK kinase inhibitor in lung cancer. Clin Cancer Res 2008; 14: 4275–4283.
30. Stemke-Hale K, Gonzalez-Angulo AM, Lluch A et al. An integrative genomic and proteomic analysis of PIK3CA, PTEN, and AKT mutations in breast cancer. Cancer Res 2008; 68: 6084–6091.
31. Hollestelle A, Elstrodt F, Nagel JH et al. Phosphatidylinositol-3-OH kinase or RAS pathway mutations in human breast cancer cell lines. Mol Cancer Res 2007; 5: 195–201.
32. Haverty PM, Fridlyand J, Li L et al. High-resolution genomic and expression analyses of copy number alterations in breast tumors. Genes Chromosomes Cancer 2008; 47: 530–542.
33. Oda K, Okada J, Timmerman L et al. PIK3CA cooperates with other phosphatidylinositol 3′-kinase pathway mutations to effect oncogenic transformation. Cancer Res 2008; 68: 8127–8136.
34. Baselga J, Albanell J, Ruiz A et al. Phase II and tumor pharmacodynamic study of gefitinib in patients with advanced breast cancer. J Clin Oncol 2005; 23: 5323–5333.
35. Mohsin SK, Weiss HL, Gutierrez MC et al. Neoadjuvant trastuzumab induces apoptosis in primary breast cancers. J Clin Oncol 2005; 23: 2460–2468.
36. Clynes RA, Towers TL, Presta LG, Ravetch JV. Inhibitory Fc receptors modulate in vivo cytotoxicity against tumor targets. Nat Med 2000; 6: 443–446.

Cancer Letters 282 (2009) 14–24

Contents lists available at ScienceDirect

Cancer Letters

journal homepage: www.elsevier.com/locate/canlet

Sensitivity of breast cancer cell lines to the novel insulin-like growth factor-1 receptor (IGF-1R) inhibitor NVP-AEW541 is dependent on the level of IRS-1 expression

Toru Mukohara [a,b,*,1], Hiroyuki Shimada [b], Naomi Ogasawara [b], Ryoko Wanikawa [b], Manami Shimomura [b], Tetsuya Nakatsura [b], Genichiro Ishii [b], Joon Oh Park [d,e], Pasi A. Jänne [e], Nagahiro Saijo [b,c], Hironobu Minami [a,b,1]

[a] Division of Oncology and Hematology, National Cancer Center Hospital East, 6-5-1 Kashiwanoha, Kashiwa 277-8577, Japan
[b] Research Center for Innovative Oncology, National Cancer Center Hospital East, 6-5-1 Kashiwanoha, Kashiwa 277-8577, Japan
[c] Division of Thoracic Oncology, National Cancer Center Hospital East, 6-5-1 Kashiwanoha, Kashiwa 277-8577, Japan
[d] Division of Hematology–Oncology, Department of Medicine, Samsung Medical Center, Sungkyunkwan University, School of Medicine, 50 Irwon-Dong, Gangnam-Gu, Seoul 135-710, Republic of Korea
[e] Lowe Center for Thoracic Oncology, Department of Medical Oncology, Dana-Farber Cancer Institute, 44 Binney Street, Boston, MA 02115, USA

ARTICLE INFO

Article history:
Received 3 June 2008
Received in revised form 27 November 2008
Accepted 25 February 2009

Keywords:
Breast cancer
IGF-1R
IRS-1
Tyrosine kinase inhibitor

ABSTRACT

To investigate the potential value of targeting insulin-like growth factor-1 receptor (IGF-1R) in breast cancer, we examined the effects of NVP-AEW541, a selective small-molecule inhibitor of the IGF-1R tyrosine kinase, in a panel of 16 breast cancer cell lines. All cell lines expressed IGF-1R, but MCF-7 expressed much higher levels of insulin receptor substrate-1 (IRS-1) than the others. NVP-AEW541 was more potent at inhibiting growth of MCF-7 cells as compared to the others (IC_{50}, 1 μM vs. ≈7 μM). Comparing MCF-7 to T47D cells, which express IGF-1R at a level identical to MCF-7 but have less than 1/30 the amount of IRS-1, NVP-AEW541 caused cell-cycle arrest at the G1–S boundary, reduced *in vitro* cell migration, and enhanced the cytotoxic effects of vinorelbine and paclitaxel in MCF-7, but not in T47D. While NVP-AEW541 decreased the phosphorylation of IGF-1R in both cell lines, it inhibited phosphorylation of Akt and disrupted the IRS-1/PI3 K complex only in MCF-7. These findings suggest that inhibiting IGF-1R may be an effective therapeutic strategy for breast cancers that co-express IGF-1R and IRS-1 at high levels.

1. Introduction

With approximately a million new cases annually, breast cancer is the leading cause of cancer death among women worldwide [1,2]. Once the disease metastasizes, it is no longer curable despite use of various systemic treatments including cytotoxic chemotherapies, endocrine manipulations, and anti-HER2 monoclonal antibodies. Therefore, novel therapeutic approaches are needed.

Since 1990s, molecularly-targeted drugs have been vigorously developed for cancer treatment. Today, receptor tyrosine kinases (RTKs) are the most promising therapeutic targets. In fact trastuzumab, an anti-HER2 monoclonal antibody used to treat HER2-overexpressing breast cancers, was one of the first therapeutic agents targeting RTKs in solid tumors. For treatment of HER2-overexpressing metastatic breast cancers, trastuzumab combined with conventional chemotherapy has significantly higher efficacy than chemotherapy alone [3]. The use of trastuzumab has recently been extended to adjuvant or neo-adjuvant

* Corresponding author. Tel.: +81 78 382 5825; fax: +81 78 382 5821.
E-mail address: mukohara@med.kobe-u.ac.jp (T. Mukohara).
[1] Present address: Department of Medical Oncology, Kobe University Hospital, 7-5-1, Kusunoki-cho, Chuo-ku, Kobe 650-0017, Japan.

0304-3835/$ - see front matter © 2009 Elsevier Ireland Ltd. All rights reserved.
doi:10.1016/j.canlet.2009.02.056

treatment for operable breast cancer [4–6]. Among other solid tumors, small-molecule tyrosine kinase inhibitors of epidermal growth factor receptor (EGFR) and Kit have provided new treatment options in patients with non-small cell lung cancer and gastrointestinal stromal tumor, respectively [7].

Insulin-like growth factor-1 receptor (IGF-1R) is another RTK characterized by its contribution to a variety of oncogenic properties, including cell proliferation, cell survival, cell motility, angiogenesis, and metastasis [8–10]. The ligands of IGF-1R are insulin-like growth factor-1 (IGF-1) and IGF-2. Once the ligands bind to IGF-1R's extracellular domain, the receptor is autophosphorylated and becomes active as a tyrosine kinase. Subsequently, adaptor molecules, such as insulin receptor substrate-1 (IRS-1) or IRS-2, are tyrosine-phosphorylated and mediate downstream signaling. This includes activation of the phosphatidylinositol 3-kinase (PI3 K)/Akt and Ras-Raf-MEK-ERK1/2 pathways [8,10]. In breast cancer cell lines, it was reported that IRS-1, but not IRS-2, is the predominant signaling molecule activated by IGF-1 [11]. Several mechanisms able to enhance the PI3 K pathway in malignancies have been identified. In breast cancer, these include mutation of p110, which is the catalytic subunit of PI3 K, and the loss of PTEN [12]. Recent studies suggested that these PI3 K-enhancing alterations may cause resistance to anti-RTK agents, such as trastuzumab and erlotinib [13–15].

Protein expression of IGF-1R is elevated in a majority of breast cancer cell lines and in 39–93% of breast cancer tumors [8,16]. Elevated levels of circulating IGF-1 have been found to be associated with an increased risk of developing breast cancer [17]. IRS-1 is reported to be frequently phosphorylated in breast cancer tumors [18] and the level of IRS-1 is correlated with shorter disease-free survival in a subgroup of breast cancer patients [19]. Further, Lu, et al. have proposed a potential mechanism of resistance to trastuzumab *in vitro*, which consists of alternative cell signaling triggered by IGF-1R instead of HER2 in the presence of trastuzumab [20]. Based on these findings, IGF-1R is considered to be a rational therapeutic target in breast cancer.

Several different methods for targeting IGF-1R are under investigation, including oligodeoxynucleotides, monoclonal antibodies, and small-molecule tyrosine kinase inhibitors [8]. Among these, small-molecule inhibitors have the advantage of possible oral administration. NVP-AEW541 is a selective inhibitor for IGF-1R tyrosine kinase [21,22]. A previous study showed that it inhibited anchorage-independent growth of MCF-7 breast cancer cells [22]. Here, as part of our investigations into protocol designs for clinical trials of NVP-AEW541 in patients with breast cancer, we evaluated the efficacy of this agent in a large panel of breast cancer cell lines, its activities against oncogenic processes other than cell growth, details of its mechanism of action, and methods for identifying tumors likely to respond to it.

In this study, we show that NVP-AEW541 inhibits cell growth and motility, and enhances the induction of apoptosis by chemotherapeutic agents *in vitro*. These effects were observed only in MCF-7 breast cancer cells, the only line among those tested that expresses both IGF-1R and IRS-1 at high level. We also showed that NVP-AEW541 inhibits Akt phosphorylation by causing dissociation of IRS-1/PI3 K complex, which appears to be an important mechanism of action. These results suggest that cells that co-express IGF-1R and IRS-1 are likely to be dependent on the signaling pathway from IGF-1R to PI3 K, and therefore sensitive to NVP-AEW541, which disrupts this pathway.

2. Materials and methods

2.1. Cell culture

MCF-7, MDA-MB-361, HCC1954, MDA-MB-453, UACC893, CAMA-1, MDA-MB-435S, ZR75-30, HCC70, and HCC1419 cell lines were purchased from the American Type Culture Collection (ATCC, Manassas, VA). BT474, SKBR-3, BT549, T47D, ZR75-1, and MDA-MB-231 cells were kindly provided by Dr. Ian Krop of the Dana-Farber Cancer Institute. MCF-7, HCC1954, MDA-MB-453, UACC893, CAMA-1, ZR75-30, HCC70, HCC1419, BT474, SKBR-3, BT549, T47D, and ZR75-1 cells were maintained in RPMI 1640 (Cellgro; Mediatech, Inc., Herndon, CA) supplemented with 10% FBS (Gemini-Bio-Products, Inc., Woodland, CA), 100 units/ml penicillin, 100 units/ml streptomycin, and 2 mM glutamine. MDA-MB-361, MDA-MB-435S, and MDA-MB-231 cells were maintained in Dulbecco's Modified Eagle's Medium (DMEM) (Cellgro) with 10% FBS, 100 units/ml penicillin, 100 units/ml streptomycin, and 2 mM glutamine.

2.2. Drugs

NVP-AEW541 was a kind gift of Novartis Pharma (Basel, Switzerland). Stock solutions were prepared in dimethyl sulfoxide (DMSO) and stored at −20 °C. The drugs were diluted in fresh media before each experiment. In all experiments, the final concentration of DMSO was less than 0.1%. The lack of effect of DMSO at this concentration on cell growth, cell migration, or cell-cycle distribution in MCF-7 and T47D was confirmed (data not shown). Vinorelbine and paclitaxel were purchased from the pharmacy of the National Cancer Center Hospital East.

2.3. Antibodies and Western blotting

Cells were lysed in lysis buffer (20 mM Tris [pH 7.5], 150 mM NaCl, 10% glycerol, 1% NP40, and 2 mM EDTA) containing protease and phosphatase inhibitors (100 mM NaF, 1 mM phenylmethylsulfonyl fluoride [PMSF], 1 mM Na_3VO_4 2 μg/ml aprotinin, and 5 μg/ml leupetin). Cell lysates were centrifuged at 14,000g relative centrifugal force (rcf) to make protein extracts. The protein extracts were separated by gel electrophoresis on 7–10% polyacrylamide gels (depending on the target's molecular weight), transferred to nitrocellulose membranes (Schleicher and Schuell, Dassel, Germany) and detected by immunoblotting using Amersham ECL™ Advance Western Blotting Detection Kit (GE Healthcare, Buckinghamshire, England). The resulting signals were quantified to obtain digital values

using a GS-800 calibrated densitometer (Bio-Rad, Hercules, CA) and Quantity One 1-D analysis software (Bio-Rad). The phospho-IGF-1R (19H7, Tyr1135/1136), IGF-1R, phospho-IRS-1 (Ser 612), IRS-1, phospho-Akt (pS473), Akt, and PTEN antibodies were purchased from Cell Signaling Technology (Beverly, MA). The phospho-ERK1/2 (pT185/pY187) and ERK1/2 antibodies were purchased from Biosource International Inc (Camarillo, CA). The p85 antibody was purchased from Upstate (Charlottesville, VA). The β-actin antibody was purchased from Sigma–Aldrich (St. Louis, MO).

2.4. Phospho-RTK array

At approximately 70% of cell confluence, protein extracts of MCF-7, T47D, HCC1954, and MDA-MB-361 cells were prepared as described in Section 2.3. The extracts were applied to a Human Phospho-RTK Array (R&D Systems, Minneapolis, MN, USA), which can detect the phosphorylation level of 42 different RTKs on the same nitrocellulose membrane. Assays were performed in accordance with the manufacturer's instructions. The resulting signals were quantified as described in Section 2.3. The intensity of each RTK's phosphorylation was represented as a percentage relative to the internal positive control. To obtain relative intensity among the 42 RTKs, the deviation value was calculated as follows: (intensity for the RTK − average intensity for 42 RTKs) × 10/standard deviation of intensities for 42 RTKs.

2.5. Immunoprecipitation

Immunoprecipitation was performed as described previously [23]. Briefly, fresh protein extracts (see Section 2.3) were incubated overnight with anti-p85 antibody. Immunoprecipitation products were washed three times with ice-cold NP-40 lysis buffer before boiling in 2× Laemmli sample buffer and analyzed by Western blotting.

2.6. Cell growth assay

Growth inhibition was assessed by use of the MTS assay (Promega, Madison, WI). This assay, a colorimetric method for determining the number of viable cells, is based on the bioreduction of 3-(4,5-dimethylthiazol-2-yl)-5-(3-carboxymethoxyphenyl)-2-(4-sulfophenyl)-2H-tetrazolium (MTS) to a soluble formazan product that is detected spectrophotometrically at a wavelength of 490 nm. Cells diluted in 160 μl/well of maintenance cell culture media (see "*Cell Culture and Reagents*") were plated in 96-well flat-bottom plates (Corning, Inc., Corning, NY). The number of cells required to obtain an optical density (OD) of 1.3–2.2, the linear range of the assay, after 96 h of growth was determined for each cell line beforehand. The number

Table 1
Baseline expression of phospho-IGF-1R, IGF-1R, phospho-IRS-1, and IRS-1 in breast cancer cells grown in 10% serum-containing media.

	Phospho-IGF-1R	IGF-1R	Phospho-IRS-1	IRS-1
BT474	0.34	0.47	0.10	0.11
BT549	0.28	0.26	0.06	0.07
CAMA-1	0.22	0.00	0.04	0.00
HCC1419	0.61	0.35	0.04	0.09
HCC1954	2.48	0.49	0.08	0.20
HCC70	0.19	0.57	0.14	0.15
MCF-7	1.00	1.00	1.00	1.00
MDA-MB-MB231	0.44	0.34	0.28	0.27
MDA-MB-MB361	1.72	0.95	0.11	0.05
MDA-MB-435S	0.54	0.85	0.11	0.10
MDA-MB-453	0.05	0.25	0.08	0.05
SKBR-3	0.86	0.41	0.01	0.02
T47D	1.15	1.10	0.03	0.03
UACC893	0.28	0.57	0.01	0.01
ZR75-1	0.25	0.96	0.09	0.24
ZR75-30	0.38	0.40	0.01	0.02

Intensity of each band measured with Western blotting for each cell line (Fig. 1) was quantified and expressed relative to that for MCF-7.

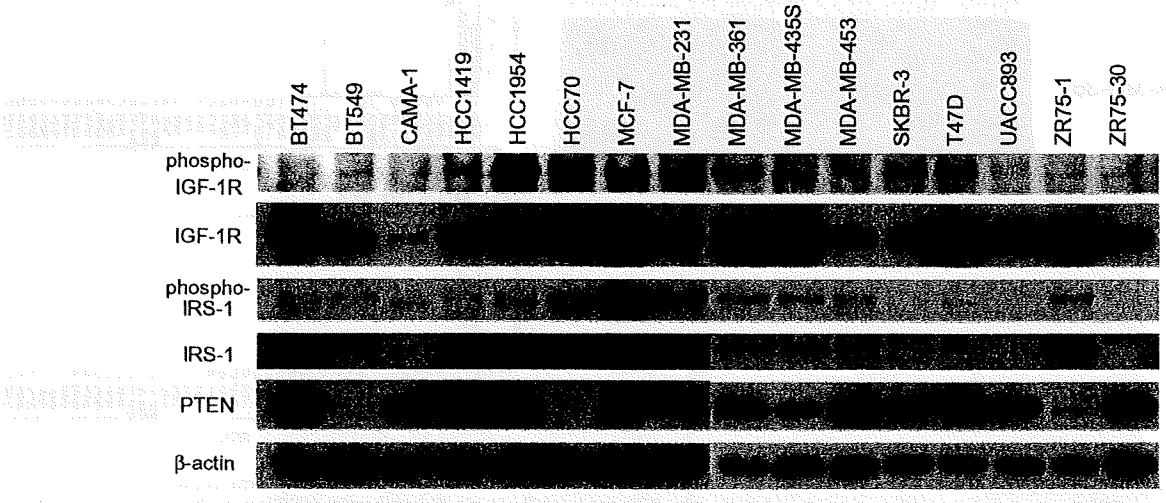

Fig. 1. Expression of phosphorylated IGF-1R, IGF-1R, phosphorylated IRS-1, IRS-1, and PTEN in breast cancer cell lines. Breast cancer cell lines grown in 10% serum-containing medium were lysed and immunoblotted for each protein. The blots were stripped and reprobed for β-actin as loading control.

of cells per well used in the subsequent experiments were as follows: MCF-7, 2000; MDA-MB-361, 8000; HCC1954, 2500; MDA-MB-453, 7000; UACC893, 7500; CAMA-1, 6000; MDA-MB-435S, 2000; ZR75-30, 7500; HCC70, 4000; HCC1419, 8000; BT474, 3000; SKBR-3, 2500; BT549, 2000; T47D, 2500; ZR75-1, 7500; and MDA-MB-231, 2500. Drugs were added 24 h after plating, and the cells were incubated for another 96 h. Wells of the plate (6–12) were set for each experimental point, and all experiments were repeated at least three times. The data are expressed as percentage of growth relative to that of untreated control cells.

2.7. FACS analysis

The FACS analysis was performed using methods similar to those described previously [24]. Briefly, 1–1.5 × 10^6 cells were seeded into 10 cm^3 plates, and the drugs were added 24 h later. After 24 h of treatment, the cells were trypsinized and fixed overnight in ethanol at 4 °C. Fixed cells were then resuspended in 0.5% RNase A (Sigma), centrifuged, resuspended in 5 μM propidium iodine (Sigma) in 38 mM sodium citrate, incubated at room temperature for 30 min, and analyzed by FACS Calibur flow cytometry (Becton Dickinson, Franklin Lakes, NJ) with a cell-cycle test software, ModFit LT™ (Verity Software House Inc., Topsham, ME). All experiments were repeated three times.

2.8. Scratch wound migration assay

Breast cancer cells were seeded in 6-well tissue culture plates (Corning, Inc.) and incubated in 10% serum-containing media until confluence. Gaps were then created by scraping cells with P1000 pipette tips and the cells were

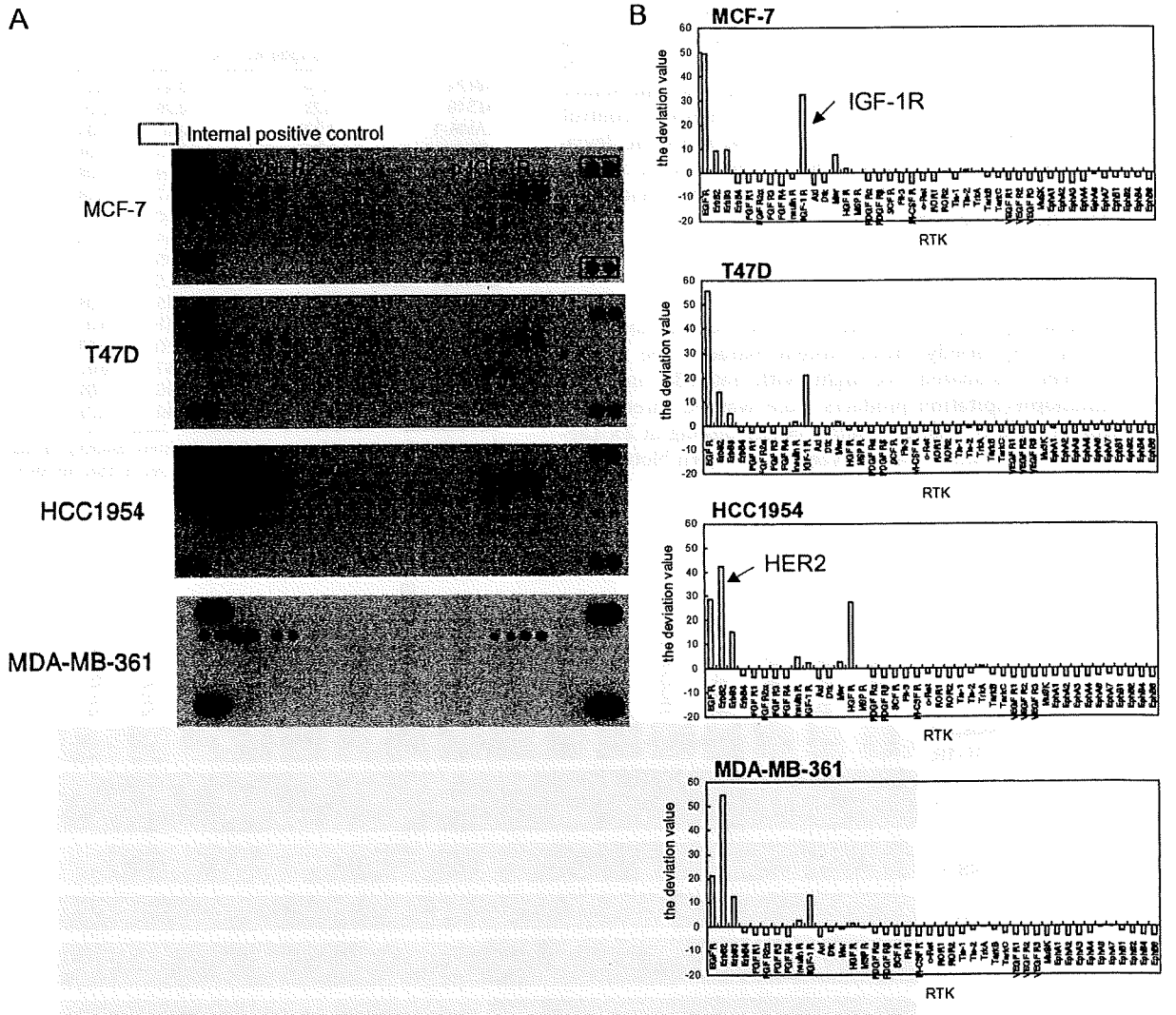

Fig. 2. Phosphorylation profile of 42 RTKs in MCF-7, T47D, HCC1954, and MDA-MB-361 breast cancer cell lines. The protein extract prepared from each cell line grown in 10% serum-containing medium was applied to phospho-RTK arrays. (A) The levels of phosphorylated RTKs in each cell line were visualized on a nitrocellulose membrane. (B) The average intensities of the dots for each phosphorylated RTK (*x*-axis) were quantified. The deviation value was calculated as described in Section 2 and plotted on the *y*-axis.

cultured in fresh media containing 10% serum with or without 1 μM NVP-AEW541. The plates were photographed at 0, 24, 48, 72, and 96 h using a microscope with a digital video camera installed (BZ-8000, Keyence, Osaka, Japan). Distance of cell migration was measured at three fixed positions (top, right middle and bottom on the screen) using BZ analyzer software (Keyence).

3. Results

3.1. Expression and phosphorylation level of IGF-1R and IRS-1 in breast cancer cell lines

Sixteen breast cancer cell lines were evaluated for the expression and phosphorylation level of IGF-1R and IRS-1 using Western blotting. All the lines expressed detectable levels of IGF-1R (Fig. 1). While a majority of them exhibited phosphorylation of IGF-1R detectable with the phospho-specific antibody, there was no clear correlation between expression level and phosphorylation of the receptor (Fig. 1 and Table 1, $p = 0.07$). On the other hand, expression and phosphorylation level of IRS-1 appeared significantly correlated with each other (Fig. 1 and Table 1, $p = 0.002$). MCF-7 cells expressed substantially more IRS-1 and phospho-IRS-1 than the other 15 cell lines, with levels at least three times those seen in other lines (Fig. 1 and Table 1). Of the 16 breast cancer cell lines, all but BT549, HCC70, and ZR75-1 expressed detectable levels of PTEN (Fig. 1).

3.2. MCF-7 and T47D have high relative phosphorylation of IGF-1R

Fifty-eight RTKs have been identified in the human genome [25], and cancer cells could potentially depend on any RTK in terms of activating downstream effectors. To shed light on the relative importance of IGF-1R among many other RTKs in breast cancer cells, we utilized a commercially available phospho-RTK array, which can detect the phosphorylation level of 42 different RTKs on one nitrocellulose membrane (see Section 2). Protein extracts obtained from MCF-7, T47D, HCC1954, and MDA-MB-361 cells, which had the highest levels of phosphorylated IGF-1R as measured by Western blotting (Fig. 1 and Table 1), were applied to the array. We quantified each phospho-RTK as described in Section 2. As shown in Fig. 2, the relative intensity of phosphorylated IGF-1R is higher in MCF-7 and T47D than in HCC1954 and MDA-MB-361. Of note, both HCC1954 and MDA-MB-361 are reported to have amplification of the HER2 gene and over-expression of the protein [26]. Consistent with this, the relative intensity of phosphorylated HER2 is high in those two cell lines (Fig. 2).

3.3. NVP-AEW541 inhibits cell growth of breast cancer cell lines

To examine the inhibitory effects of NVP-AEW541 on cell growth, cells were cultured in 10% serum-containing media with various concentrations of NVP-AEW541 (3.3 nM to 10 μM). As seen in Fig. 3, NVP-AEW541 inhibits cell growth of MCF-7 more potently than that of the other breast cancer cell lines (IC_{50} for MCF-7 vs. the other cell lines, 1 μM vs. approximately. 7 μM).

Taken together, neither expression nor phosphorylation of IGF-1R predicts sensitivity to NVP-AEW541. This is shown by comparison of the MCF-7 and T47D cell lines, which showed different sensitivities to NVP-AEW541 despite equivalency in expression and phosphorylation level of IGF-1R (Figs. 1 and 3, and Table 1). In addition, those two cell lines have very similar phospho-RTK profiles as shown in Fig. 2. On the other hand, IRS-1 expression and phosphorylation levels are much higher in MCF-7 cells than in T47D cells (Fig. 1 and Table 1). To explore the role of IRS-1 in the mechanism of action of NVP-AEW541, we therefore decided to compare MCF-7 with T47D in further experiments. Because NVP-AEW541 can inhibit many other kinases, especially insulin receptor, at concentrations above 2 μM [22], we could not exclude the possibility that growth inhibition observed at 3.3 μM or higher might be due to non-specific effects. Therefore, we used 1 μM or lower concentrations of NVP-AEW541 in subsequent experiments.

3.4. NVP-AEW541 alters cell-cycle distribution

FACS analysis was used to determine the effect of NVP-AEW541 on MCF-7 and T47D cell cycling. In MCF-7 cells, treatment with 1 μM NVP-AEW541 led to an increase in the G1–G0 fraction along with a decrease in the G2–M and S fractions, indicating cell-cycle arrest at the G1–S boundary (Fig. 4A). In contrast, very little change in cell-cycle distribution was observed in T47D cells (Fig. 4B). NVP-AEW541 produced no increase

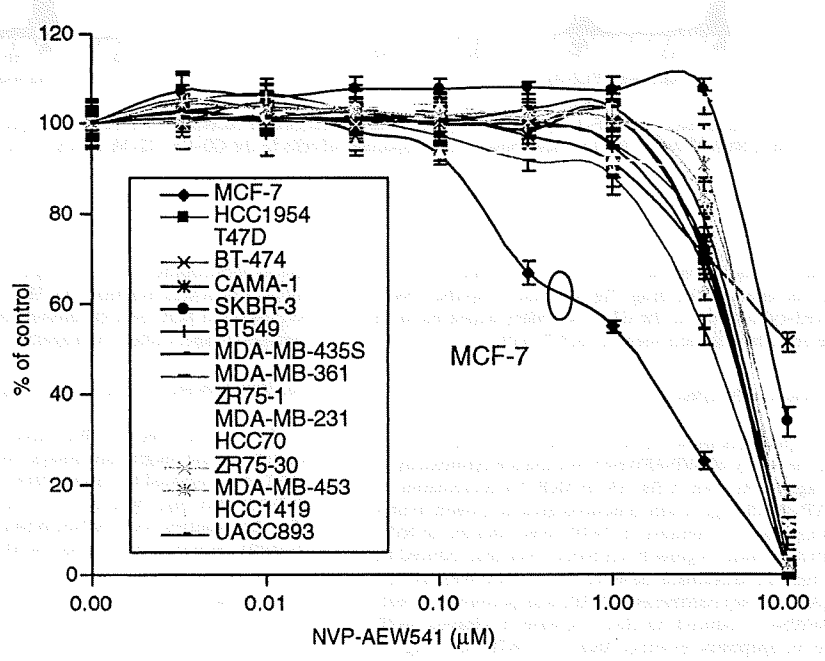

Fig. 3. Growth inhibitory effect of NVP-AEW541 on breast cancer cells. Breast cancer cells are grown in 10% serum-containing media for 5 days in the presence of various concentrations of NVP-AEW541. Percentage of viable cells is shown relative to that of untreated control (*y*-axis). The *x*-axis shows the concentration of NVP-AEW541. Each data point represents the mean value and standard deviation of 6–12 replicate wells.

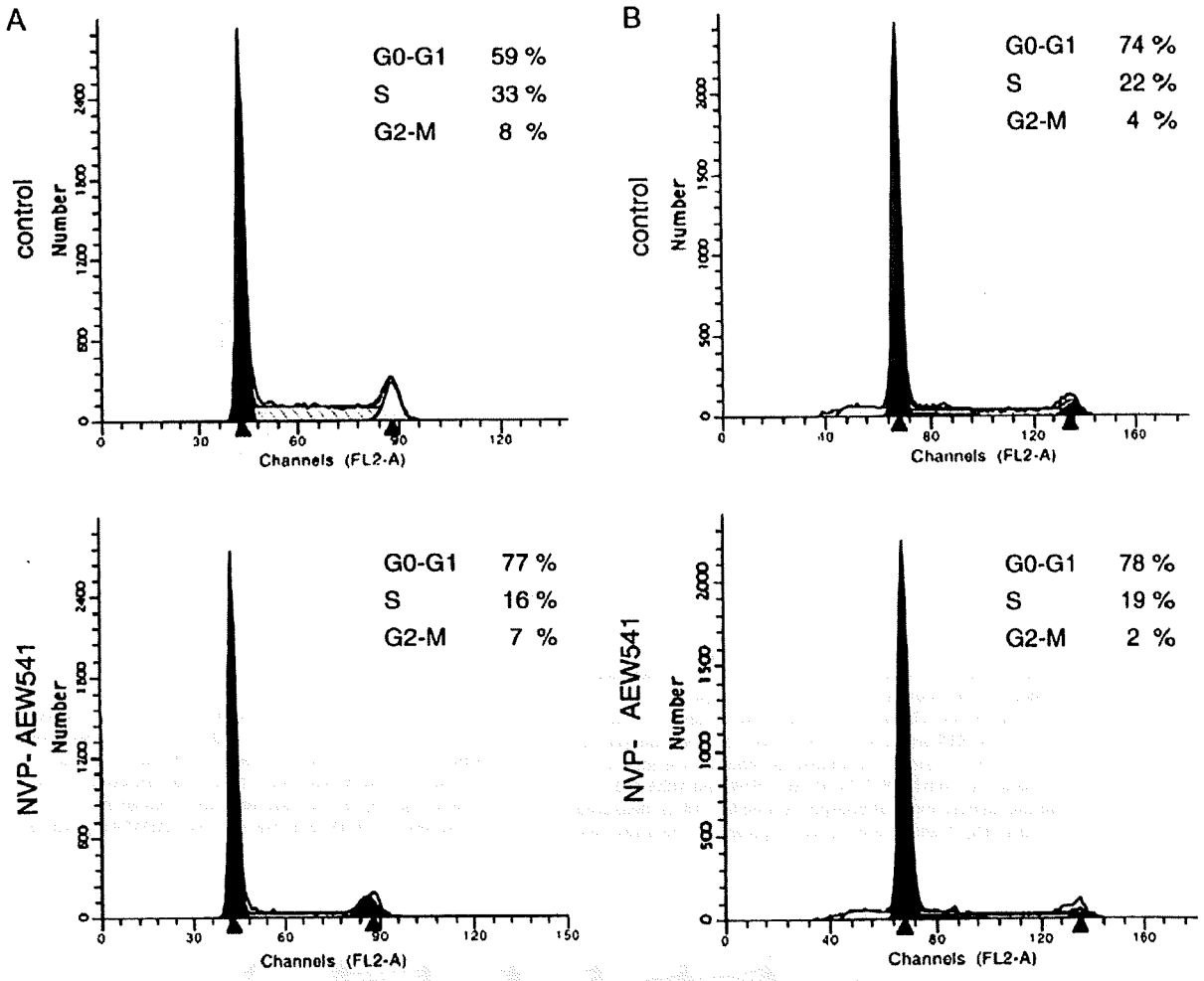

Fig. 4. Change in cell-cycle parameters in MCF-7 (A) and T47D (B) cells as a result of NVP-AEW541 treatment. Examples of FACS analysis of cells that were treated with 0 and 1 μM of NVP-AEW541 for 24 h are shown. The proportion of cells in the G0–G1, G2–M, and S phases of the cell-cycle are shown on top right hand corner.

in the sub-G1 fraction, indicative of apoptosis, in either cell line, suggesting a cytostatic effect of the drug (Fig. 4). Taken together, NVP-AEW541-induced cell-cycle arrest at the G1–S boundary appeared to be responsible for the growth inhibition seen in MCF-7 cells.

3.5. NVP-AEW541 enhances the effect of chemotherapeutic drugs

Because IGF-1R signaling is known to be important for cell survival [8], we next examined the ability of NVP-AEW541 to enhance cytotoxicity of chemotherapeutic agents. As seen in Fig. 5A, in MCF-7 a combination of vinorelbine and NVP-AEW541 generally produced greater growth inhibition than either drug alone. In contrast, in T47D cells, addition of NVP-AEW541 caused little increase in growth inhibition over that induced by vinorelbine alone (Fig. 5B). To evaluate the level of apoptosis, Western blot analysis for poly (ADP-ribose) polymerase (PARP) was performed. Treatment with NVP-AEW541 produced no clear increase in cleaved PARP, which is indicative for apoptosis, in either MCF-7 or T47D cells (Fig. 5C and D), consistent with the cytostatic effect indicated by FACS analysis. Treatment with vinorelbine caused an increase in cleaved PARP in both cell lines (Fig. 5C and D). In MCF-7 cells, the addition of NVP-AEW541 to vinorelbine caused a further increase, suggesting that the compound enhances vinorelbine-induced apoptosis (Fig. 5C), but in T47D cells the enhancement was minimal (Fig. 5D). Similar results were observed when NVP-AEW541 was used in combination with paclitaxel, another chemotherapeutic agent often used against breast cancer (data not shown).

3.6. NVP-AEW541 inhibits migration of MCF-7 cells

To test the effect of NVP-AEW541 on cell motility, we performed scratch wound migration assays. Without NVP-AEW541, MCF-7, and T47D cells migrated at similar rates over 96 h. Treatment with 1 μM of NVP-AEW541 significantly reduced the rate of migration in MCF-7 (Fig. 6A, control vs. NVP-AEW541 at 72 and 96 h, $p = 0.001$ and $P < 0.001$, respectively) but not T47D cells (Fig. 6B).

3.7. NVP-AEW541 inhibits IGF-1R signaling in MCF-7

We next examined changes in phosphorylation of IGF-1R and representative downstream signaling molecules in MCF-7 and T47D cells grown in 10% serum media with or without 1 μM NVP-AEW541. In both cell lines, NVP-AEW541 inhibited phosphorylation of IGF-1R (Fig. 7A). Baseline phospho-IRS-1 was much higher in MCF-7 cells than in T47D,

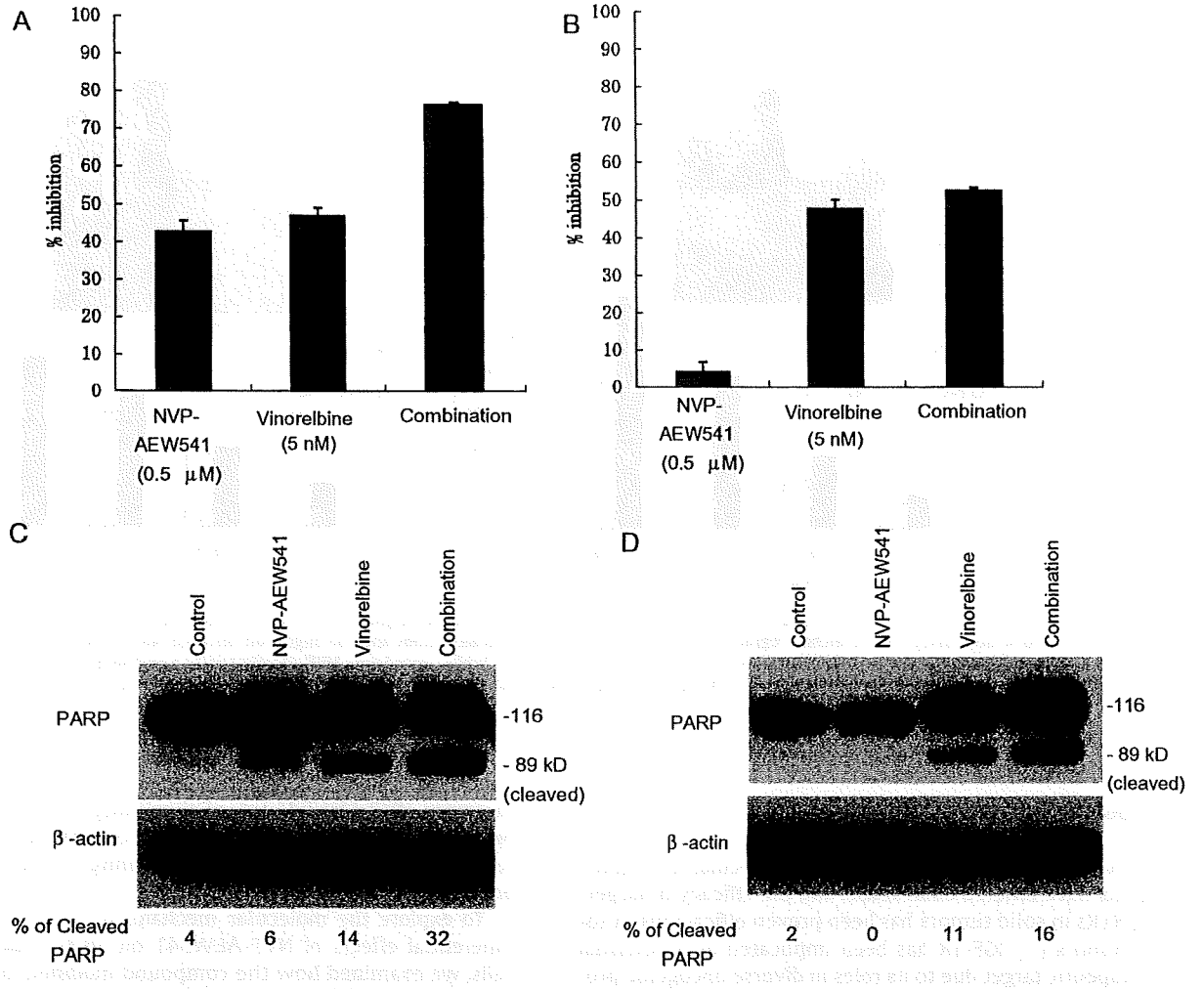

Fig. 5. Effect of NVP-AEW541 on vinorelbine-induced apoptosis in MCF-7. MCF-7 (A and C) and T47D (B and D) cell lines were treated with 0.5 μM of NVP-AEW541, 5 nM of vinorelbine, and their combination. (A and B) Viable cells were quantified by the MTS assay and are expressed as a percentage relative to untreated controls (*y*-axis). Each data point represents the mean value and standard deviation of 6–12 replicate wells. (C and D) Western blot for PARP with MCF-7 and T47D grown in the absence or presence of 0.5 μM of NVP-AEW541, 5 nM of vinorelbine, and their combination. The blot was stripped and reprobed for β-actin as a loading control. Percentage of the cleaved form (89-kDa) was quantified and is shown at the bottom of the blots.

and was inhibited by NVP-AEW541 (Fig. 7A). This inhibition coincided with a decrease in phosphorylation of Akt (Fig. 7A). In contrast, the level of phospho-Akt in T47D cells was much higher than in MCF-7 and was decreased only slightly by NVP-AEW541 (Fig. 7A). Phosphorylation of ERK1/2 was not affected NVP-AEW541 in either cell line, nor was the total amount of any of these signaling proteins (Fig. 7A). To test the effects of NVP-AEW541 on ligand-dependent cell signaling, we serum-starved MCF-7 and T47D cells overnight and stimulated them with IGF-1 for 15 min with or without 2 h pre-exposure to 1 μM NVP-AEW541, then analyzed lysates of the cells by Western blotting (Fig. 7B). In both cell lines, phosphorylation of IGF-1R dramatically increased with the IGF-1 stimulation, and was significantly inhibited by NVP-AEW541 pre-treatment. Interestingly, in MCF-7 cells phosphorylation of IRS-1 was observed even without ligand-stimulation, and was increased by addition of IGF-1 (Fig. 7B). NVP-AEW541 inhibited the IGF-1-dependent phosphorylation of IRS-1 and phosphorylation of Akt in MCF-7 cells (Fig. 7B). In T47D, in contrast, IRS-1 phosphorylation was barely detectable and did not change with addition of IGF-1 or NVP-AEW541 (Fig. 7B). Accordingly, the level of Akt phosphorylation changed only slightly (Fig. 7B). On the other hand, while phosphorylation of ERK1/2 was increased by IGF-1 and inhibited by NVP-AEW541 in T47D cells, it was unaffected in MCF-7 (Fig. 7B).

Taken together, these results indicate that inhibition of cells' proliferation, cell-cycle progression, survival, and motility by NVP-AEW541 does not correlate with inhibition of IGF-1R phosphorylation, but rather with decreased phosphorylation of Akt. The role of the ERK1/2 pathways appeared relatively small when compared to the PI3 K pathways, at least for the oncogenic properties we tested.

3.8. NVP-AEW541 disrupts IRS-1/PI3 K complex

In activating PI3 K, IGF-1R is known to utilize IRS-1 as a scaffold protein [10]. Because inhibition of the PI3 K pathway appeared to play an important role in the mechanism of action of NVP-AEW541, we next examined the effect of the compound on the interaction between IRS-1 and p85. MCF-7 and T47D cells were treated with or without 1 μM NVP-AEW541 for 24 h, and cellular protein extracts were immunoprecipitated with p85 antibody and analyzed by immunoblotting with IRS-1 and p85 antibodies. As shown in Fig. 7C, IRS-1 and p85 are physically associated in MCF-7 cells and this association is disrupted by NVP-AEW541. In contrast, the two proteins are not associated in T47D cells. These findings are consistent with our Western blot analysis showing that NVP-AEW541 suppresses phosphorylation of Akt in MCF-7 but not in T47D (Fig. 7A and B).

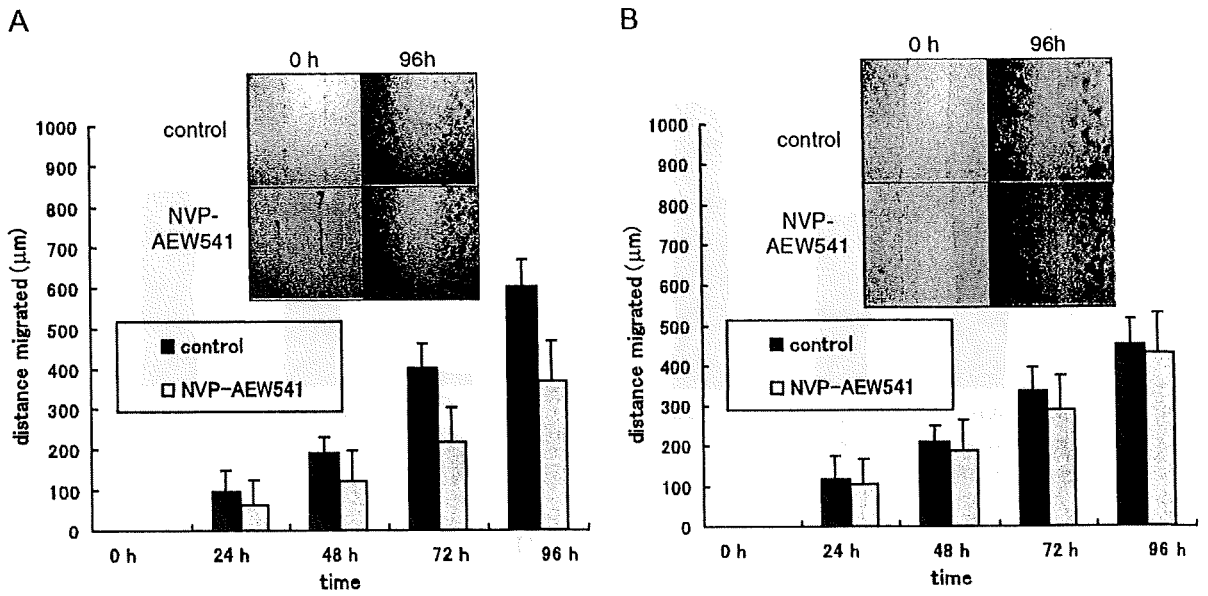

Fig. 6. Inhibitory effect of NVP-AEW541 on migration of MCF-7. MCF-7 and T47D cell lines were grown to confluence and treated with 1 μM NVP-AEW541 before an *in vitro* scratch assay. The scratched region was photographed at the indicated times and the migration distance was measured at three fixed positions (top, middle, and bottom). (A) The migration is significantly slower in MCF-7 cells treated with NVP-AEW541 at 72 h and 96 h ($P < 0.05$). Each data point represents the mean and standard deviation of 6–12 replicate wells. (B) In T47D cell line, NVP-AEW541 produces no significant change in the rate of migration.

4. Discussion

Over the last decade, a number of molecularly-targeted agents have entered clinical use, and the efficacy of targeting RTKs in solid tumors has been proven efficacious in solid tumors [7]. IGF-1R has been implicated as a potential therapeutic target due to its roles in diverse oncogenic processes including cell proliferation, survival, motility, and metastasis [10]. In the present study, we examined *in vitro* effects of selectively inhibiting IGF-1R with NVP-AEW541.

We first found that even though all 16 of the breast cancer cell lines tested express IGF-1R, and many of them show baseline phosphorylation of this RTK, one cell line, MCF-7, was much more sensitive to NVP-AEW541 than the others in assays of cell growth. Interestingly, we found that of the 16 cell lines, only MCF-7 has high expression and phosphorylation of both IGF-1R and its substrate IRS-1 (Fig. 1 and Table 1). We hypothesized that concurrent expression and phosphorylation of both proteins could play a role in the mechanism of action of NVP-AEW541. To test this hypothesis we chose to compare MCF-7 and T47D cells, because these lines had identical expression and phosphorylation levels of IGF-1R, and almost identical profiles of other phospho-RTKs (Fig. 2), but differ in that MCF-7 cells have much higher expression and phosphorylation of IRS-1 (Fig. 1 and Table 1).

We found that in MCF-7 but not in T47D, 1 μM NVP-AEW541 causes G1–S cell-cycle arrest, consistent with the higher growth inhibition observed in MCF-7. We also found that in MCF-7 but not in T47D, NVP-AEW541 enhanced the cytotoxicity of vinorelbine and paclitaxel. Furthermore, NVP-AEW541 retarded cell migration in MCF-7 but not T47D. These observations are consistent with the reported contribution of IGF-1R signaling to the cellular processes measured in these assays.

To explore the molecular mechanisms underlying the differential effects of NVP-AEW541 on MCF-7 and T47D cells, we examined how the compound modified different cell signaling pathways. In MCF-7 but not T47D cells, 1 μM NVP-AEW541 significantly inhibited Akt phosphorylation, both in the presence of 10% serum and after serum starvation followed by IGF-1 treatment (Fig. 7). In contrast, NVP-AEW541 did not affect the ERK pathway, another well-characterized proliferation and survival pathway, in cells of either line grown in 10% serum. Furthermore, we demonstrated that NVP-AEW541 dissociated IRS-1/PI3 K in MCF-7 but not in T47D cells. These findings suggest that cellular sensitivity to NVP-AEW541 is determined by whether the signaling axis of IGF-1R–IRS-1–PI3 K is functional. The presence of the axis may be indicated by high expression of both IGF-1R and IRS-1, as discussed below. Alternatively, dissociation of IGF-1R and IRS-1 may be naturally present in some cancer cells, because in T47D stimulation with IGF-1 caused only a small increase in phosphorylation of IRS-1 (Fig. 7B). The PI3 K/Akt pathway is known to be multifunctional, mediating important oncogenic processes such as cell proliferation, cell survival, and cell motility [27]. This is again consistent with the present findings that NVP-AEW541 inhibited not only cell growth but other oncogenic properties in MCF-7.

Considering therapeutic implications, our results suggest that measuring IGF-1R expression alone provides insufficient information to select tumors sensitive to

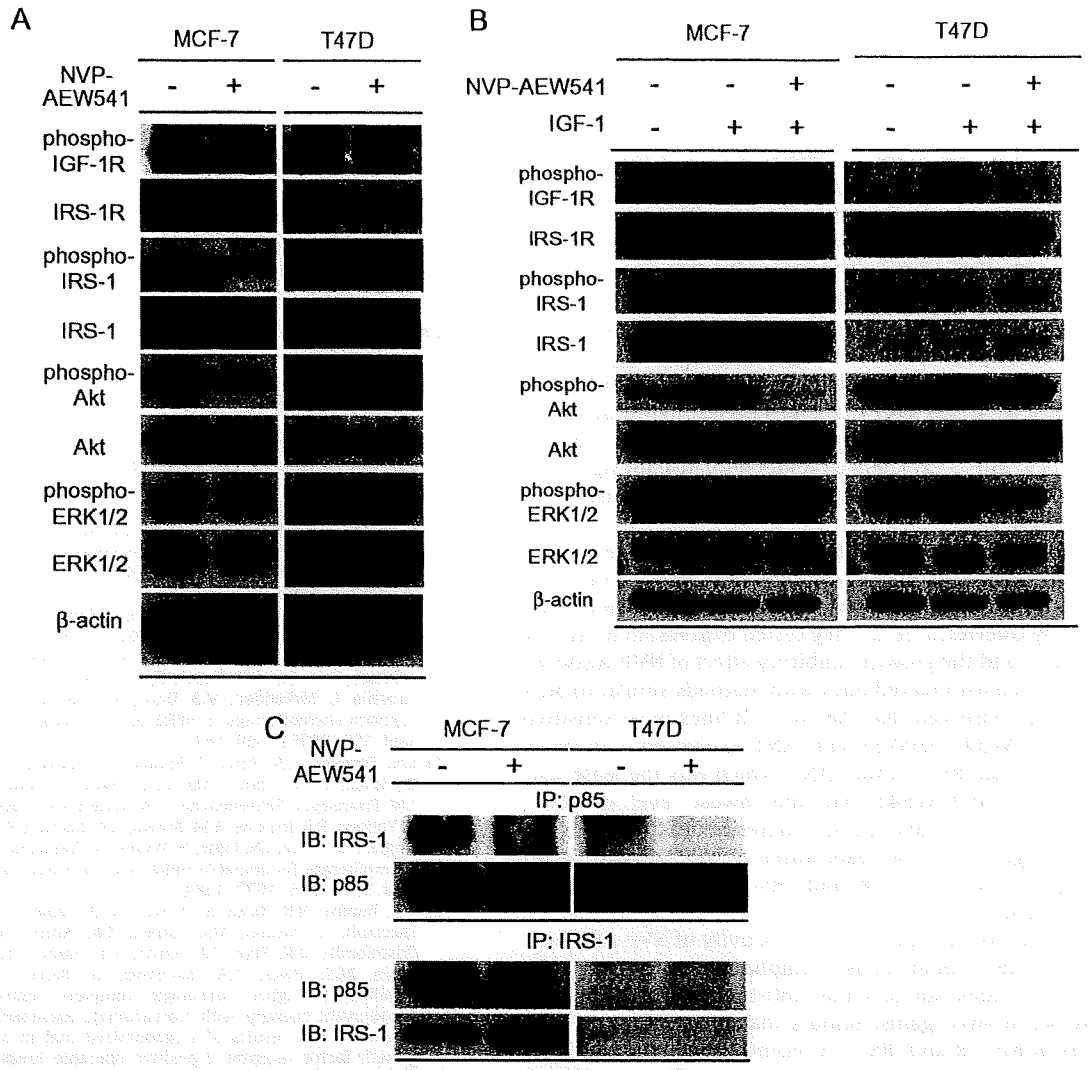

Fig. 7. Effects of NVP-AEW541 on phosphorylation of IGF-1R and downstream signaling molecules. (A) MCF-7 and T47D cell lines were treated with 1 μM NVP-AEW541 for 24 h and the levels of phosphorylated IGF-1R, Akt, and ERK1/2 were assessed using phospho-specific antibodies for each protein. The blot was stripped and reprobed with an antibody detecting the total form of the protein, and again with antibody for β-actin as loading control. (B) Effects of IGF-1 and NVP-AEW541 on phosphorylation of IGF-1R and downstream Akt and ERK1/2. MCF-7 and T47D cells were serum starved overnight and then grown in the presence or absence of 1 μM NVP-AEW541 for 2 h followed by IGF-1 (50 ng/ml) stimulation for 15 min. Western blots are shown for phospho- and total IGF-1R, Akt, and ERK1/2. (C) MCF-7 and T47D cell lines were grown in the presence or absence of NVP-AEW541 for 24 h. Protein extracts (500 μg) were immunoprecipitated with an anti-p85 antibody and subjected to immunoblot assays with anti-IRS-1 and anti-p85 antibodies. In MCF-7, the association of IRS-1 and p85 is significantly diminished in the presence of NVP-AEW541.

NVP-AEW541, consistent with a previous study by Scotlandi et al. using musculoskeletal cancer cell lines [21]. Our results rather suggest that the presence of high IRS-1 expression beside IGF-1R expression indicates the presence of a signaling axis from IGF-1R to PI3 K, and would thus be informative for selecting NVP-AEW541-sensitive tumors. This concept is supported by a recent study by Byron, et al. [28]. In the study, they showed that in T47D-YA breast cancer cells expressing active IGF-IR but lacking IRS-1, IGF-1 did not stimulate cell proliferation but did when cDNA constructs encoding human IRS-1 were stably transfected into the cells [28]. They also showed that MCF-7 cells with IRS-1 knocked down by means of interfering RNA (siRNA) exhibited diminished IGF-1-stimulated cell growth compared to parental cells [28]. Despite the high frequency of IRS-1 expression in breast cancer specimens reported in a previous study [29], 69.7%, the definition and the frequency of over-expression of IRS-1 remains unclear. If the level of IRS-1 MCF-7 shows should be regarded as over-expression, it may be infrequent in breast cancer. It also remains unknown how frequent IGF-1R and IRS-1 simultaneously over-express in breast cancer. However, because a previous study showed that higher levels of IRS-1 predicted worse disease-free survival after curative surgery in a subset of breast cancer patients [19], NVP-AEW541 might be efficacious against relatively aggressive tumors.

In T47D cells, phosphorylation of Akt is high even after serum starvation (Fig. 7B), suggesting the presence of a

mechanism causing constitutive activity of the PI3 K pathway. One possible candidate is an activating mutation of p110 (H1047R in exon 20) in T47D [30]. Interestingly, however, MCF-7 is also reported to have an activating mutation in p110, though at a different site (E545 K in exon 9) [30]. We confirmed the presence of these mutations in each cell line for ourselves (data not shown). Both mutations have been shown to cause equal elevation of PI3 K catalytic activity when expressed in a normal mammary epithelial cell line [31]. However, our data showed that phosphorylation of Akt in the absence of serum is much lower in MCF-7 than T47D cells, and is boosted by addition of exogenous IGF-1 (Fig. 7B), which suggests that these two mutations may have different effects in cancer cell lines in which they occur endogenously. In addition, it is of therapeutic importance to know that cells with mutant PI3 K, like MCF-7, still depend on up-stream signals in terms of PI3 K activation, and therefore can be sensitive to anti-RTK drugs.

Our study has some limitations. First, the use of only one cell line with high sensitivity to NVP-AEW541 precludes generalization of the results. In a recently published study by Guerreiro, et al., they tested expression of IGF-1R and IRS-1 and the growth inhibitory effect of NVP-AEW541 for 9 neuroblastoma cell lines with methods similar to ours [32]. They observed that the two cell lines most sensitive to NVP-AEW541, SHSY5Y and LAN1, expressed high levels of IGF-1R and IRS-1, while LAN5, which was the least sensitive to NVP-AEW541, had the lowest level of IRS-1. Although the authors did not address the issue, their results suggest that the association of NVP-AEW541 with co-expression of IGF-1R and IRS-1 may be a general phenomenon.

Second, we did not test *in vivo* activity of NVP-AEW541. Because IGF-1 could act as a lymphangiogenic factor [33], our result does not preclude anti-tumor effects of NVP-AEW541 *in vivo* against tumors that are unlike MCF-7 in terms of IGF-1R and IRS-1. A recently published study by Tanno and colleagues showed *in vivo* efficacy of NVP-AEW541 for neuroblastoma cell lines, but they were shown to be sensitive *in vitro* as well [34]. Therefore, it remains to be addressed, and is a focus of our ongoing study, whether NVP-AEW541 can work *in vivo* especially for cancer cells that are insensitive *in vitro*.

In summary, our study supports the possibility of targeting IGF-1R in breast cancer. Inhibiting IGF-1R and consequently the PI3 K/Akt pathway is therapeutically attractive as it may not only inhibit cell growth but also enhance the effect of chemotherapeutic agents and reduce the ability of cells to migrate to other sites. However, *in vitro* effects of IGF-1R receptor inhibition in breast cancer cells appeared to be limited to those that express both IGF-1R and IRS-1 at high levels. Although the validity of the findings in our study should be evaluated in clinical trials, they could potentially lead to individualized use of NVP-AEW541 in breast cancer.

Conflict of interest statement

None declared.

Acknowledgements

This study is supported by a Grant from Foundation for Promotion of Cancer Research, Japan (T.M.), Start-up Research Grant for Young Investigators from Japan Society for the Promotion of Science (T.M.), Grant-in-Aid for Young Scientists (B) from the Ministry of Education, Culture, Sports, Science and Technology, Japan (T.M.), and Grants-in-Aid for Cancer Research from the Ministry of Health, Labour and Welfare, Japan (H.M. and N.S.).

References

[1] K. McPherson, C.M. Steel, J.M. Dixon, ABC of breast diseases, breast cancer-epidemiology, risk factors, and genetics, BMJ 321 (2000) 624–628.
[2] D.M. Parkin, F. Bray, J. Ferlay, P. Pisani, Global cancer statistics, 2002, CA Cancer J. Clin. 55 (2005) 74–108.
[3] D.J. Slamon, B. Leyland-Jones, S. Shak, H. Fuchs, V. Paton, A. Bajamonde, T. Fleming, W. Eiermann, J. Wolter, M. Pegram, J. Baselga, L. Norton, Use of chemotherapy plus a monoclonal antibody against HER2 for metastatic breast cancer that overexpresses HER2, New Engl. J. Med. 344 (2001) 783–792.
[4] M.J. Piccart-Gebhart, M. Procter, B. Leyland-Jones, A. Goldhirsch, M. Untch, I. Smith, L. Gianni, J. Baselga, R. Bell, C. Jackisch, D. Cameron, M. Dowsett, C.H. Barrios, G. Steger, C.S. Huang, M. Andersson, M. Inbar, M. Lichinitser, I. Lang, U. Nitz, H. Iwata, C. Thomssen, C. Lohrisch, T.M. Suter, J. Ruschoff, T. Suto, V. Greatorex, C. Ward, C. Straehle, E. McFadden, M.S. Dolci, R.D. Gelber, Trastuzumab after adjuvant chemotherapy in HER2-positive breast cancer, New Engl. J. Med. 353 (2005) 1659–1672.
[5] E.H. Romond, E.A. Perez, J. Bryant, V.J. Suman, C.E. Geyer Jr., N.E. Davidson, E. Tan-Chiu, S. Martino, S. Paik, P.A. Kaufman, S.M. Swain, T.M. Pisansky, L. Fehrenbacher, L.A. Kutteh, V.G. Vogel, D.W. Visscher, G. Yothers, R.B. Jenkins, A.M. Brown, S.R. Dakhil, E.P. Mamounas, W.L. Lingle, P.M. Klein, J.N. Ingle, N. Wolmark, Trastuzumab plus adjuvant chemotherapy for operable HER2-positive breast cancer, New Engl. J. Med. 353 (2005) 1673–1684.
[6] A.U. Buzdar, N.K. Ibrahim, D. Francis, D.J. Booser, E.S. Thomas, R.L. Theriault, L. Pusztai, M.C. Green, B.K. Arun, S.H. Giordano, M. Cristofanilli, D.K. Frye, T.L. Smith, K.K. Hunt, S.E. Singletary, A.A. Sahin, M.S. Ewer, T.A. Buchholz, D. Berry, G.N. Hortobagyi, Significantly higher pathologic complete remission rate after neoadjuvant therapy with trastuzumab, paclitaxel, and epirubicin chemotherapy: results of a randomized trial in human epidermal growth factor receptor 2-positive operable breast cancer, J. Clin. Oncol. 23 (2005) 3676–3685.
[7] D.S. Krause, R.A. Van Etten, Tyrosine kinases as targets for cancer therapy, New Engl. J. Med. 353 (2005) 172–187.
[8] Y.H. Ibrahim, D. Yee, Insulin-like growth factor-I and breast cancer therapy, Clin. Cancer. Res. 11 (2005) 944s–950s.
[9] Y. Feng, Z. Zhu, X. Xiao, V. Choudhry, J.C. Barrett, D.S. Dimitrov, Novel human monoclonal antibodies to insulin-like growth factor (IGF)-II that potently inhibit the IGF receptor type I signal transduction function, Mol. Cancer Ther. 5 (2006) 114–120.
[10] M.N. Pollak, E.S. Schernhammer, S.E. Hankinson, Insulin-like growth factors and neoplasia, Nat. Rev. Cancer 4 (2004) 505–518.
[11] J.G. Jackson, M.F. White, D. Yee, Insulin receptor substrate-1 is the predominant signaling molecule activated by insulin-like growth factor-I, insulin, and interleukin-4 in estrogen receptor-positive human breast cancer cells, J. Biol. Chem. 273 (1998) 9994–10003.
[12] R.L. Dillon, D.E. White, W.J. Muller, The phosphatidyl inositol 3-kinase signaling network: implications for human breast cancer, Oncogene 26 (2007) 1338–1345.
[13] I.K. Mellinghoff, M.Y. Wang, I. Vivanco, D.A. Haas-Kogan, S. Zhu, E.Q. Dia, K.V. Lu, K. Yoshimoto, J.H. Huang, D.J. Chute, B.L. Riggs, S. Horvath, L.M. Liau, W.K. Cavenee, P.N. Rao, R. Beroukhim, T.C. Peck, J.C. Lee, W.R. Sellers, D. Stokoe, M. Prados, T.F. Cloughesy, C.L. Sawyers, P.S. Mischel, Molecular determinants of the response of glioblastomas to EGFR kinase inhibitors, New Engl. J. Med. 353 (2005) 2012–2024.
[14] Y. Nagata, K.H. Lan, X. Zhou, M. Tan, F.J. Esteva, A.A. Sahin, K.S. Klos, P. Li, B.P. Monia, N.T. Nguyen, G.N. Hortobagyi, M.C. Hung, D. Yu, PTEN activation contributes to tumor inhibition by trastuzumab, and

loss of PTEN predicts trastuzumab resistance in patients, Cancer Cell 6 (2004) 117–127.
[15] K. Berns, H.M. Horlings, B.T. Hennessy, M. Madiredjo, E.M. Hijmans, K. Beelen, S.C. Linn, A.M. Gonzalez-Angulo, K. Stemke-Hale, M. Hauptmann, R.L. Beijersbergen, G.B. Mills, M.J. van de Vijver, R. Bernards, A functional genetic approach identifies the PI3K pathway as a major determinant of trastuzumab resistance in breast cancer, Cancer Cell 12 (2007) 395–402.
[16] C. Shimizu, T. Hasegawa, Y. Tani, F. Takahashi, M. Takeuchi, T. Watanabe, M. Ando, N. Katsumata, Y. Fujiwara, Expression of insulin-like growth factor 1 receptor in primary breast cancer: immunohistochemical analysis, Hum. Pathol. 35 (2004) 1537–1542.
[17] S.E. Hankinson, W.C. Willett, G.A. Colditz, D.J. Hunter, D.S. Michaud, B. Deroo, B. Rosner, F.E. Speizer, M. Pollak, Circulating concentrations of insulin-like growth factor-I and risk of breast cancer, Lancet 351 (1998) 1393–1396.
[18] Q. Chang, Y. Li, M.F. White, J.A. Fletcher, S. Xiao, Constitutive activation of insulin receptor substrate 1 is a frequent event in human tumors: therapeutic implications, Cancer Res. 62 (2002) 6035–6038.
[19] R.L. Rocha, S.G. Hilsenbeck, J.G. Jackson, C.L. VanDenBerg, C. Weng, A.V. Lee, D. Yee, Insulin-like growth factor binding protein-3 and insulin receptor substrate-1 in breast cancer: correlation with clinical parameters and disease-free survival, Clin. Cancer Res. 3 (1997) 103–109.
[20] Y. Lu, X. Zi, Y. Zhao, D. Mascarenhas, M. Pollak, Insulin-like growth factor-I receptor signaling and resistance to trastuzumab (Herceptin), J. Natl. Cancer Inst. 93 (2001) 1852–1857.
[21] K. Scotlandi, M.C. Manara, G. Nicoletti, P.L. Lollini, S. Lukas, S. Benini, S. Croci, S. Perdichizzi, D. Zambelli, M. Serra, C. Garcia-Echeverria, F. Hofmann, P. Picci, Antitumor activity of the insulin-like growth factor-I receptor kinase inhibitor NVP-AEW541 in musculoskeletal tumors, Cancer. Res. 65 (2005) 3868–3876.
[22] C. Garcia-Echeverria, M.A. Pearson, A. Marti, T. Meyer, J. Mestan, J. Zimmermann, J. Gao, J. Brueggen, H.G. Capraro, R. Cozens, D.B. Evans, D. Fabbro, P. Furet, D.G. Porta, J. Liebetanz, G. Martiny-Baron, S. Ruetz, F. Hofmann, In vivo antitumor activity of NVP-AEW541-A novel, potent, and selective inhibitor of the IGF-IR kinase, Cancer Cell 5 (2004) 231–239.
[23] J.A. Engelman, P.A. Janne, C. Mermel, J. Pearlberg, T. Mukohara, C. Fleet, K. Cichowski, B.E. Johnson, L.C. Cantley, ErbB-3 mediates phosphoinositide 3-kinase activity in gefitinib-sensitive non-small cell lung cancer cell lines, Proc. Natl. Acad. Sci. USA 102 (2005) 3788–3793.
[24] T. Mukohara, G. Civiello, I.J. Davis, M.L. Taffaro, J. Christensen, D.E. Fisher, B.E. Johnson, P.A. Janne, Inhibition of the met receptor in mesothelioma, Clin. Cancer Res. 11 (2005) 8122–8130.
[25] G. Manning, D.B. Whyte, R. Martinez, T. Hunter, S. Sudarsanam, The protein kinase complement of the human genome, Science 298 (2002) 1912–1934.
[26] M. Lacroix, G. Leclercq, Relevance of breast cancer cell lines as models for breast tumours: an update, Breast Cancer Res. Treat. 83 (2004) 249–289.
[27] M. Hanada, J. Feng, B.A. Hemmings, Structure, regulation and function of PKB/AKT–a major therapeutic target, Biochim. Biophys. Acta 1697 (2004) 3–16.
[28] S.A. Byron, K.B. Horwitz, J.K. Richer, C.A. Lange, X. Zhang, D. Yee, Insulin receptor substrates mediate distinct biological responses to insulin-like growth factor receptor activation in breast cancer cells, Br. J. Cancer 95 (2006) 1220–1228.
[29] M. Koda, M. Sulkowska, L. Kanczuga-Koda, S. Sulkowski, Expression of insulin receptor substrate 1 in primary breast cancer and lymph node metastases, J. Clin. Pathol. 58 (2005) 645–649.
[30] L.H. Saal, K. Holm, M. Maurer, L. Memeo, T. Su, X. Wang, J.S. Yu, P.O. Malmstrom, M. Mansukhani, J. Enoksson, H. Hibshoosh, A. Borg, R. Parsons, PIK3CA mutations correlate with hormone receptors, node metastasis, and ERBB2, and are mutually exclusive with PTEN loss in human breast carcinoma, Cancer Res. 65 (2005) 2554–2559.
[31] S.J. Isakoff, J.A. Engelman, H.Y. Irie, J. Luo, S.M. Brachmann, R.V. Pearline, L.C. Cantley, J.S. Brugge, Breast cancer-associated PIK3CA mutations are oncogenic in mammary epithelial cells, Cancer Res. 65 (2005) 10992–11000.
[32] A.S. Guerreiro, D. Boller, T. Shalaby, M.A. Grotzer, A. Arcaro, Protein kinase B modulates the sensitivity of human neuroblastoma cells to insulin-like growth factor receptor inhibition, Int. J. Cancer 119 (2006) 2527–2538.
[33] M. Bjorndahl, R. Cao, L.J. Nissen, S. Clasper, L.A. Johnson, Y. Xue, Z. Zhou, D. Jackson, A.J. Hansen, Y. Cao, Insulin-like growth factors 1 and 2 induce lymphangiogenesis in vivo, Proc. Natl. Acad. Sci. USA 102 (2005) 15593–15598.
[34] B. Tanno, C. Mancini, R. Vitali, M. Mancuso, H.P. McDowell, C. Dominici, G. Raschella, Down-regulation of insulin-like growth factor I receptor activity by NVP-AEW541 has an antitumor effect on neuroblastoma cells in vitro and in vivo, Clin. Cancer Res. 12 (2006) 6772–6780.

Jpn J Clin Oncol 2009;39(2)116–123
doi:10.1093/jjco/hyn135

Phase I Dose-escalation and Pharmacokinetic Trial of Lapatinib (GW572016), a Selective Oral Dual Inhibitor of ErbB-1 and -2 Tyrosine Kinases, in Japanese Patients with Solid Tumors

Kazuhiko Nakagawa[1], Hironobu Minami[2,†], Masayuki Kanezaki[3], Akihira Mukaiyama[3], Yoshiyuki Minamide[3], Hisao Uejima[1], Takayasu Kurata[1], Toshiji Nogami[1], Kenji Kawada[2], Hirofumi Mukai[2], Yasutsuna Sasaki[4] and Masahiro Fukuoka[1]

[1]Kinki University School of Medicine, Osaka, [2]National Cancer Center Hospital East, Chiba, [3]GlaxoSmithKline, Tokyo and [4]Saitama Medical School, Saitama, Japan

Received August 24, 2008; accepted October 30, 2008; published online December 3, 2008

Objective: The Phase I dose-escalation study was conducted to evaluate the safety and pharmacokinetics of lapatinib (GW572016), a dual ErbB-1 and -2 inhibitor, in Japanese patients with solid tumors that generally express ErbB-1 and/or overexpress ErbB-2.
Methods: Patients received oral lapatinib once daily until disease progression or in an event of unacceptable toxicity.
Results: Twenty-four patients received lapatinib at dose levels of 900, 1200, 1600 and 1800 mg/day; six subjects enrolled to each dose level. The majority of drug-related adverse events was mild (Grade 1–2); the most common events were diarrhea (16 of 24; 67%), rash (13 of 24; 54%) and dry skin (8 of 24; 33%). No Grade 4 adverse event was observed. There were four Grade 3 drug-related adverse events in three patients (i.e. two events of diarrhea at 1600 and 1800 mg/day each and γ-glutamyl transpeptidase increase at 1800 mg/day). The maximum tolerated dose was 1800 mg/day. The pharmacokinetic profile of lapatinib in Japanese patients was comparable to that of western subjects.
Conclusions: Lapatinib was well tolerated at doses of 900–1600 mg/day in Japanese solid tumor patients. Overall, our findings were similar to those of overseas studies.

Key words: ErbB-1 – ErbB-2 – lapatinib – phase I – tyrosine kinase inhibitor

INTRODUCTION

Dysregulation of the human epidermal growth factor (ErbB) family of cell surface receptors has been noted in several solid tumors. Binding of extracellular ligand to ErbB receptors activates multiple intracellular signaling pathways that can promote tumor growth through processes, such as cell proliferation, differentiation and inhibition of apoptosis. ErbB-1 and ErbB-2 are implicated in the pathogenesis of several cancers (1), and their overexpression in epithelial tumors—including those of the lung, breast, head and neck, colon, stomach, ovary and prostate—often correlates with poor prognosis (2,3).

ErbB receptors present two rational targets for inhibition: blockade of the extracellular ligand-binding domain by monoclonal antibodies and inhibition of the intracellular tyrosine kinase domain by small molecules (4). Several anticancer agents target specific ErbB isoforms. For example, the small molecule tyrosine kinase inhibitors gefitinib (Iressa®) and erlotinib (Tarceva®) and the monoclonal antibody cetuximab (Erbitux®) all target ErbB-1 (5–7), and thus, they are indicated for the treatment of non-small cell lung cancer (NSCLC) and colorectal cancer (8,9). Furthermore, a monoclonal antibody directed against ErbB-2 (trastuzumab, Herceptin®) has been approved for patients with ErbB-2-overexpressing breast cancer (10). Sensitivity to some of these agents is strongly associated with the expression levels of ErbB-1 and -2 (2,3).

For reprints and all correspondence: Kazuhiko Nakagawa, Kinki University School of Medicine, 377-2 Ohnohigashi, Osakasayama, Osaka 589-0014, Japan. E-mail: nakagawa@med.kindai.ac.jp

†Present address: Kobe University Hospital and Graduate School of Medicine, Hyogo, Japan

Since it has been suggested that tumors with ErbB-1 expression and ErbB-2 overexpression are more aggressive than those without expression of the receptors (11–13), it has been proposed that dual inhibition of ErbB-1 and -2 could be a useful approach in patients with overexpression of these receptors. Lapatinib (GW572016) is a potent, orally active, small molecule dual inhibitor of ErbB-1 and -2. Lapatinib markedly reduces autophosphorylation of ErbB-1 and -2, and inhibits activation of Erk1/2 and AKT, the downstream effectors of cell proliferation and cell survival, respectively (14–17). Lapatinib inhibits tumor cell proliferation in various human tumor cell lines expressing ErbB-1 and overexpressing ErbB-2, as well as in tumor xenograft models (14–17).

Preclinical study of lapatinib revealed the agent to be well tolerated with an effective half-life of ~24 h, suggesting once-daily oral administration to be feasible (18). Clinical studies of the safety and efficacy of lapatinib in cancer patients are underway.

This was the first Japanese Phase I study of lapatinib in patients with solid tumors. This study was primarily designed to assess the safety of repeated oral doses of lapatinib in these patients and to investigate pharmacokinetics to see if they are comparable with those in western patients.

PATIENTS AND METHODS

Study Design

This was a non-randomized, open-label, multicenter, dose-escalation Phase I study conducted at two sites in Japan—Kinki University Hospital, Osaka and National Cancer Center Hospital East, Chiba.

The primary objectives were to assess the safety of repeated oral doses of lapatinib, to determine the maximum tolerated dose (MTD) in patients with solid tumors, to evaluate the pharmacokinetics (PK) of repeated oral doses of lapatinib and to compare the data from overseas studies and based on these data, to find the clinically recommended dose of lapatinib in Japanese patients enrolled in further studies.

Patient Eligibility

Adult patients aged 20–74 years with histologically or cytologically confirmed solid tumors that are generally known to express EGFR and/or overexpress ErbB-2 (including colorectal cancer, gastric cancer, NSCLC and breast cancer) were eligible for inclusion, provided that they had failed standard therapies or there were no other appropriate therapies available (19–40). Patients had to have normal function of major organs and adequate bone marrow, hepatic and renal functions defined as hemoglobin $\geq$9 g/dl, neutrophil count $\geq$1500/mm^3 and platelets $\geq$100 000/mm^3, AST and ALT $\leq$2.5 of upper limit of normal (ULN) and bilirubin $\leq$1.5 of ULN, and serum creatinine $\leq$1.5 of ULN, respectively. Left ventricular ejection fraction by echocardiography had to be $\geq$50% and in all patients an appropriate length of time since cessation of previous therapy was required (chemotherapy, radiotherapy, surgery or investigational products other than anticancer drugs, $\geq$4 weeks; nitrosourea compounds or mitomycin C, $\geq$6 weeks; biologic response modifiers or hormone therapy, $\geq$2 weeks). Patients were also to have an Eastern Cooperative Oncology Group performance status (PS) 0–2 and life expectancy $\geq$3 months after the start of lapatinib treatment.

Exclusion criteria were serious complications (Grade $\geq$3 according to the National Cancer Institute common toxicity criteria, NCI-CTC, version 2); pleural effusion, ascites and/or pericardial effusion requiring drainage by puncture, intracavital administration, or any other relevant treatment; systematic steroid use for $\geq$50 days or possible need for long-term use of systemic steroids; multiple active cancers; symptomatic brain metastases; malabsorption and/or total resection of the stomach or small intestine; corneal disorder; history of drug allergy; breast feeding; previous trastuzumab-induced impaired cardiac function; and previous acute pulmonary disorder or interstitial pneumonia induced by gefitinib.

All patients gave written informed consent before the start of study. The protocol was approved by the institutional review board of each study site. The study was conducted according to the World Medical Association Declaration of Helsinki (41) and Japanese good clinical practice guidelines (42).

Treatment

Based on the findings of overseas Phase I study (43), and in order to compare PK profiles with an overseas parallel Phase I study (44), patients were assigned to receive lapatinib 900, 1200 or 1600 mg/day for 21 consecutive days. Lapatinib was taken orally once daily with water after a light low-fat breakfast, except on Days 1 and 21 when it was administered in fasting state.

The dose levels started at 900 mg/day and increased to 1200 and 1600 mg/day, then increased by 200-mg increments until MTD was reached. MTD was defined as the dose at which dose-limiting toxicity (DLT), i.e. a drug-related adverse event of NCI-CTC Grade $\geq$3, occurred within 21 days after the initiation of dosage in two or more patients at each dose level with six subjects. When DLT was observed, the next dose for the patients was to be postponed, and could not restart until NCI-CTC grade became $\leq$2 within 14 days. In such cases, when NCI-CTC became Grade 2 or below, the dose was to be restarted at the previous dose level. When NCI-CTC did not reach Grade 2 or below after dose delays of 14 days, the treatment for the patients was to be discontinued. These dose delays and reductions were allowed to be performed only once.

Although appropriate supportive care and symptomatic treatment were allowed, prophylactic use (including

antiemetics) was not permitted between screening and Day 21 of the treatment period. Anticancer therapy of any kind, medications that may affect the absorption or metabolism of lapatinib, and other investigational drugs were prohibited throughout the study. Also, to prevent PK interactions, patients were instructed to avoid grapefruit, grapefruit juice and St John's Wort (*Hypericum perforatum*) throughout the study.

Safety Assessments

Assessments including clinical laboratory tests, vital signs, PS and body weight were performed at screening, at baseline (i.e. within 3 days before the first dose), on Days 7, 14 and 21, every 4 weeks thereafter, on cessation of treatment, and on the last day of observation (i.e. 28 days after the final dose or immediately before the start of next anticancer therapy). Chest X-ray, 12-lead electrocardiogram and echocardiography were performed at screening, once between Days 14 and 21, and on the last observation day. Toxicity was graded according to the NCI-CTC version 2.

Pharmacokinetic Analysis

For PK evaluation, 3-ml blood samples were collected at 1 h pre-dosing and at 1, 2, 3, 4, 6, 8, 10, 12 and 24 h after dosing on Days 1 and 21 and at pre-dosing on Days 7 and 14. Urine samples were collected before dosing on Day 1 and 0–24 h after dosing on Days 1 and 21.

Serum concentrations of lapatinib were measured by liquid chromatography tandem mass spectrometry with a lower limit of quantitation of 1 ng/ml.

The calculated PK parameters were maximum serum concentration (C_{max}), time to C_{max} (t_{max}), area under the plasma drug concentration–time curve from 0 to 24 h (AUC_{0-24}) and terminal half-life ($t_{1/2}$). Renal clearance was calculated from urine concentrations of lapatinib.

Efficacy Assessments

For efficacy assessment [i.e. tumor response as determined by X-ray, computed tomography (CT), magnetic resonance imaging (MRI) and/or other objective measurements according to the Response Evaluation Criteria in Solid Tumors (RECIST) guidelines (45)], evaluations were performed at screening (i.e. 4 weeks before the first dose of lapatinib), once during Days 14–21, every 4 weeks thereafter, and on the last day of observation. Target and non-target lesions were assessed in the same manner before and after dosing. Consistency of efficacy evaluation by the study investigators was assessed by extramural review committee.

RESULTS

Patients

Twenty-four patients were enrolled; all had received prior chemotherapy. Table 1 shows their baseline characteristics. The median age was 60 years (range, 37–73), and they had a median PS of 1. NSCLC was the main tumor type. Six patients at four dose levels, 900, 1200, 1600 and 1800 mg/day each, received lapatinib. Eight patients received lapatinib for >3 months and four for >6 months.

All patients completed the initial 21-day treatment period, although one of the patients had dose reduction (overall compliance, 90.5%) due to the onset of a Grade 3 drug-related adverse event (diarrhea) during this period. Four patients (three at 1200 mg dose level and one at 1600 mg dose level) withdrew from study due to disease progression and four (one each at 900 and 1600 mg dose level and two at 1800 mg dose level) were withdrawn at their own request. Mean durations of study treatment in the 900, 1200, 1600 and 1800 mg groups were 131, 68.2, 117 and 49.3 days, respectively. No patient withdrew due to adverse events.

Safety

All 24 patients were eligible for safety analysis. Table 2 lists the drug-related adverse events experienced by ≥20% of

Table 1. Baseline characteristics of patients

Characteristic	Dose (mg/day)				Total ($n = 24$)
	900 ($n = 6$)	1200 ($n = 6$)	1600 ($n = 6$)	1800 ($n = 6$)	
Sex					
Male	5	2	3	4	14
Female	1	4	3	2	10
Tumor type					
Non-small cell lung cancer	5	3	1	4	13
Adenocarcinoma	2	1	1	3	7
Squamous cell carcinoma	2	1	0	1	4
Other	1	1	0	0	2
Colorectal cancer	1	1	2	1	5
Breast cancer	0	0	2	0	2
Others	0	2	1	1	4
Performance status[a]					
0	2	1	2	3	8
1	4	5	3	3	15
2	0	0	1	0	1

[a]Eastern Cooperative Oncology Group performance status.

Table 2. No. of patients with drug-related adverse events that occurred in ≥20% of patients receiving lapatinib

	Dose (mg/day)[a]												No. of patients (%)
	900			1200			1600			1800			
Common terminology criteria grade	1	2	3	1	2	3	1	2	3	1	2	3	
Any adverse events	3	3	0	4	2	0	1	4	1	2	2	2	24 (100)
Gastrointestinal	1	1	0	4	0	0	2	3	1	3	1	2	18 (75)
Diarrhea	1	1	0	4	0	0	2	1	1	3	1	2	16 (67)
Stomatitis	0	0	0	1	0	0	1	2	0	1	0	0	5 (21)
Skin	4	2	0	3	1	0	4	2	0	4	2	0	22 (92)
Rash	1	0	0	4	0	0	1	2	0	3	2	0	13 (54)
Dry skin	5	0	0	2	0	0	1	0	0	0	0	0	8 (33)
Seborrheic dermatitis	3	1	0	0	0	0	0	0	0	1	0	0	5 (21)
Paronychia	0	1	0	0	1	0	2	0	0	1	0	0	5 (21)
Metabolism and nutrition	1	0	0	1	0	0	2	0	0	4	0	0	8 (33)
Anorexia	0	0	0	1	0	0	1	0	0	3	0	0	5 (21)
Investigations	2	1	0	3	2	0	3	1	0	3	1	1	17 (71)
Decreased lymphocyte count	0	1	0	1	1	0	0	1	0	1	0	0	5 (21)

[a]Six patients at each dose level.

patients at each dose level. The majority of events was mild (Grade 1–2); the most common events were skin reactions (mostly rash and dry skin) observed in 22 patients (92%) and gastrointestinal disorders (mostly diarrhea) in 18 patients (75%). The most severe drug-related adverse events were Grade 3 diarrhea observed in one patient at 1600 mg dose level and two patients at 1800 mg dose level. One of these also had Grade 3 γ-GTP increase. All diarrhea resolved with routine symptomatic treatment during or after withdrawal of lapatinib therapy, γ-GTP increase resolved without further treatment after completion of lapatinib therapy.

Grade 1/2 drug-related nausea and vomiting were experienced only by patients at higher dose levels of lapatinib [1/6 (17%) at 1600 mg/day and 3/6 (50%) at 1800 mg/day], with Grade 2 symptoms only seen at the 1800 mg dose level.

For other adverse events, no clear drug relation was found. The most frequent events included decreased body weight and serum alkaline phosphatase increase, each observed in 10 patients (42%). Grade 1 drug-related decreases in left ventricular ejection fraction were found in three of the six patients at the 1200 mg dose level. No clinically relevant changes in vital signs, 12-lead electrocardiogram or echocardiography were noted.

Hypoxemia and pneumonia were reported at the 900-mg dose level in another patient with NSCLC on Day 35. After hypoxemia occurred, the patient continued to receive study drug medication until Day 40. We attributed hypoxemia to bronchostenosis caused by the primary disease. Oxygen inhalation and erythromycin were given and hypoxemia improved while the pneumonia was resolved on Day 41 before the patient died from progression of primary disease 3 months after the events were resolved. Chest X-rays and CT findings for this patient were inconsistent with those for interstitial pneumonia associated with other tyrosine kinase inhibitors; therefore a drug relation with lapatinib was denied.

Maximum Tolerated Dose

Dose escalation was stopped at 1800 mg/day, where two patients experienced DLT (Grade 3 diarrhea). One of these patients also experienced Grade 3 γ-GTP increase. Thus, 1800 mg/day was determined as the MTD.

Pharmacokinetics

Table 3 shows the PK parameters derived from data on 23 patients (data from one patient received lapatinib for only 19 days and are not included).

Serum concentrations of lapatinib at each dose level on Days 1 and 21 are shown in Fig. 1. Repeated doses of lapatinib (900–1800 mg/day) for 21 days resulted in dose-related increases in mean C_{max} (range, 1715–3111 ng/ml) and mean AUC_{0-24} (range, 25 680–51 099 ng·h/ml) (Table 3). Large inter-patient variations were found in mean C_{max} and mean AUC_{0-24}. After a single dose of lapatinib, t_{max} was ~4 h, although values varied greatly among patients. After 21 days of treatment, t_{max} values were similar to those observed after the single dosing on Day 1.